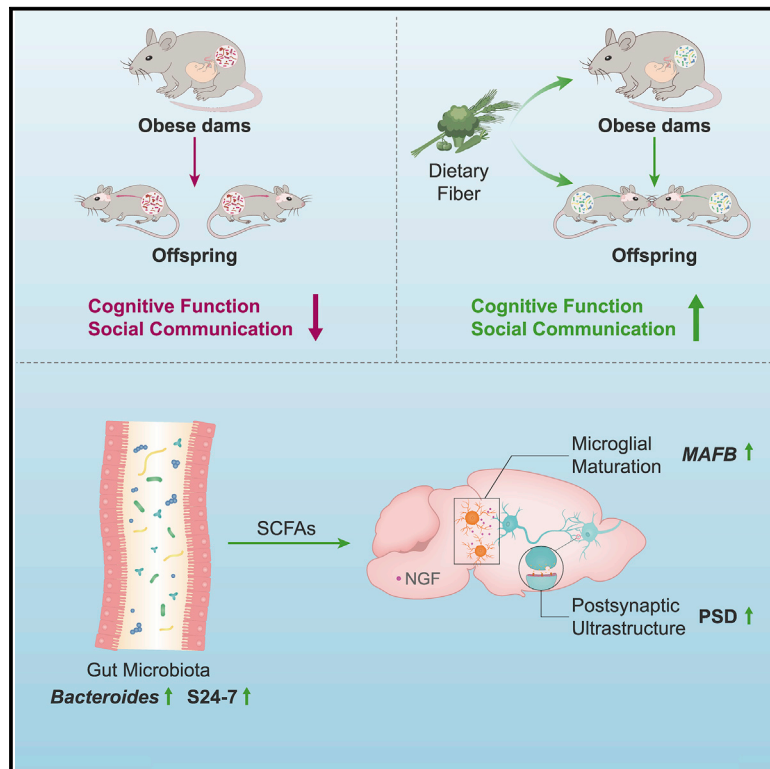


Cell Metabolism

High-fiber diet mitigates maternal obesity-induced cognitive and social dysfunction in the offspring via gut-brain axis

Graphical Abstract



Authors

Xiaoning Liu, Xiang Li, Bing Xia, ...,
Min Hou, Zhigang Liu, Xuebo Liu

Correspondence

minhou@sjtu.edu.cn (M.H.),
zhigangliu@nwsuaf.edu.cn (Z.L.),
xueboliu@nwsuaf.edu.cn (X.L.)

In brief

Maternal obesity is related to neurodevelopmental disorders in the offspring. Liu and colleagues demonstrate that maternal obesity is strongly associated with children's lower cognition and sociality. A high-fiber diet restores maternal obesity-induced behavioral disorders via mediating gut microbiota-SCFA-brain axis and improving synaptic impairments and microglial maturation defects in the offspring.

Highlights

- Maternal obesity is associated with cognition and sociality decline of children
- Maternal or offspring's high-fiber diet prevents offspring's behavioral disorders
- High-fiber diet alleviates synaptic impairments and microglial maturation defects
- Microbiota-SCFA-brain axis mediates maternal obesity-induced behavioral disorders



Article

High-fiber diet mitigates maternal obesity-induced cognitive and social dysfunction in the offspring via gut-brain axis

Xiaoning Liu,^{1,7} Xiang Li,^{1,7} Bing Xia,¹ Xin Jin,² Qianhui Zou,¹ Zhenhua Zeng,¹ Weiyang Zhao,³ Shikai Yan,¹ Ling Li,¹ Shufen Yuan,¹ Shancen Zhao,² Xiaoshuang Dai,² Fei Yin,⁴ Enrique Cadenas,⁵ Rui Hai Liu,³ Beita Zhao,¹ Min Hou,^{6,*} Zhigang Liu,^{1,3,*} and Xuebo Liu^{1,8,*}

¹College of Food Science and Engineering, Northwest A&F University, Yangling 712100, Shaanxi, China

²BGI Institute of Applied Agriculture, BGI-Shenzhen, Shenzhen 518120, Guangdong, China

³Department of Food Science, Cornell University, Ithaca, NY 14853, USA

⁴Center for Innovation in Brain Science and Department of Pharmacology, University of Arizona, Tucson, AZ 85721, USA

⁵Pharmacology and Pharmaceutical Sciences, School of Pharmacy, University of Southern California, Los Angeles, CA 90089, USA

⁶School of Public Health, College of Medicine, Shanghai Jiaotong University, Shanghai 200025, China

⁷These authors contributed equally

⁸Lead contact

*Correspondence: minhou@sjtu.edu.cn (M.H.), zhigangliu@nwsuaf.edu.cn (Z.L.), xueboliu@nwsuaf.edu.cn (X.L.)

<https://doi.org/10.1016/j.cmet.2021.02.002>

SUMMARY

Maternal obesity has been reported to be related to neurodevelopmental disorders in the offspring. However, the underlying mechanisms and effective interventions remain unclear. This cross-sectional study with 778 children aged 7–14 years in China indicated that maternal obesity is strongly associated with children's lower cognition and sociality. Moreover, it has been demonstrated that maternal obesity in mice disrupted the behavior and gut microbiome in offspring, both of which were restored by a high-fiber diet in either dams or offspring via alleviating synaptic impairments and microglial maturation defects. Co-housing and feces microbiota transplantation experiments revealed a causal relationship between microbiota and behavioral changes. Moreover, treatment with the microbiota-derived short-chain fatty acids also alleviated the behavioral deficits in the offspring of obese dams. Together, our study indicated that the microbiota-metabolites-brain axis may underlie maternal obesity-induced cognitive and social dysfunctions and that high dietary fiber intake could be a promising intervention.

INTRODUCTION

The prevalence of obesity in women of reproductive age is increasing worldwide due to the intake of high-calorie, low-fiber diets, the consumption of manufactured high-sugar foods, and a sedentary lifestyle (Hanson et al., 2017; Poston et al., 2016). Maternal obesity before and during pregnancy is widely recognized to have short-term and long-term adverse health outcomes for both mothers and their children. Evidence from both animal and human studies has shown that maternal obesity can lead to higher risks of diabetes, hypertension, and behavioral changes in the offspring (Drake and Reynolds, 2010; Godfrey et al., 2017; Harris et al., 2020), which indicates that maternal obesity may be one of the “developmental origins of health and disease” (Drake and Reynolds, 2010). The high prevalence of maternal obesity means that the determination of any such long-term effects is now an urgent priority (Heslehurst et al., 2010). Recent nationwide longitudinal studies in the UK and the US have shown that there is an increased risk of lower cognitive outcomes and autism spectrum disorders (ASDs) in children

of mothers with obesity before pregnancy (Basatemur et al., 2013; Pugh et al., 2015). Recent work in rodents has also shown that a maternal high-fat diet (mHFD) induces long-term cognitive deficits that span across several generations (Sarker and Peleg-Raibstein, 2018). Despite the potential public health importance, few cohort studies have examined the neurobiological mechanism underlying the impact of maternal obesity on offspring behavior and brain function.

A non-genetic yet heritable contributor to behavior may be the gut microbiota, which is the community of microorganisms harbored in the gastrointestinal tract that influence the development and function of the immune, metabolic, and nervous systems (Cho and Blaser, 2012; Moeller et al., 2018; Sandoval-Motta et al., 2017). The gut ecosystem is thought to be established at or soon after birth and facilitated by vertical transmission and exposure to and/or ingestion of environmental flora (Ferretti et al., 2018; Yassour et al., 2018). Thus, the influences of maternal nutrition status on the offspring's microbiome are significant and may alter mental impairment risk. Indeed, maternal obesity has been associated with alterations in the gut microbiome in the offspring,



Table 1. Participant characteristics and social competence among children

Characteristics	Maternal pre-pregnancy BMI			p Value	β (95%CI) ^c	p Value ^c
	Underweight (BMI < 18.5) (n = 132)	Normal (BMI 18.5–23.9) (n = 533)	Overweight and obese ^{a,b} (BMI > 23.9) (n = 79)			
Child's age (years) (mean \pm SD) ^a	10.32 \pm 2.01	10.39 \pm 1.86	10.42 \pm 1.95	0.955	–	–
Gender ^b : male, %	52.3	47.3	49.4	0.941	–	–
Child's BMI ^b				0.012	–	–
Underweight, %	15.4	11.6	15.9			
Normal, %	73.2	69.1	53.6			
Overweight and obese, %	11.4	19.4	30.4			
Breast feeding ^a	81.8	82.7	79.7	0.801	–	–
Maternal education level ^b				0.001	–	–
Secondary high school or lower, %	8.3	14.8	36.7			
High School, %	30.3	19.9	15.2			
Diploma in higher education or bachelor's degree, %	59.1	63.8	48.1			
Master's degree or higher, %	2.3	1.5	0.0			
Maternal pregnant weight gain (mean \pm SD) ^a	15.70 \pm 5.97	14.24 \pm 5.51	11.57 \pm 6.10	0.000	–	–
Family income (RMB) ^b					–	–
<80,000, %	5.3	9.6	27.8	0.000	–	–
80,000–150,000, %	33.3	32.5	32.9			
150,000–300,000, %	39.4	39.0	30.4			
>300,000, %	21.9	19.0	8.9			
Children's social competence (mean \pm SD)						
Total	17.05 \pm 4.06	17.10 \pm 3.72	15.65 \pm 3.79*	0.005 ^a	–0.08 (–1.89 to –0.02)	0.046
Activities	4.89 \pm 2.36	4.90 \pm 2.18	4.36 \pm 2.21	0.147 ^a	–0.05 (–0.90 to 0.20)	0.207
Social subjects	6.80 \pm 2.00	6.78 \pm 1.87	6.16 \pm 1.92*	0.045 ^a	–0.07 (–0.92 to 0.05)	0.076
School performance	5.36 \pm 0.63	5.43 \pm 0.67	5.13 \pm 0.95*	0.013 ^a	–0.07 (–0.33 to 0.01)	0.068

OR, odds ratio; CI, confidence

intervals. *Significantly different from each normal maternal pre-pregnancy BMI at $p < 0.05$.^aKruskal-Wallis test^b χ^2 test^cModel was adjusted for child's sex (male or female), child's weight status (underweight, normal weight, or overweight/obesity), family income (<80,000 RMB, 80,000–150,000 RMB, 150,000–300,000 RMB, >300,000 RMB), maternal educational level (secondary high school or lower, high school, diploma in higher education or bachelor's degree, master's degree, or higher), father's educational level (secondary high school or lower, high school, diploma in higher education or bachelor's degree, master's degree, or higher), maternal overweight/obesity versus maternal normal weight.

in both human and non-human primates (Batterham et al., 2002; Chu et al., 2016). A recent study with *Macaca fuscata* (Japanese macaque) reported that an mHFD, but not obesity, re-constructed the offspring's intestinal microbiome (Ma et al., 2014). Specifically, maternal obesity negatively impacted a subset of bacteria in the offspring gut, and selective re-introduction of *Lactobacillus* restored social deficits in offspring (Buffington et al., 2016). Another recent study also identified differences between patients with Alzheimer's disease and normal controls in 11 genera from the feces and 11 genera from the blood (Li et al., 2019). Given the emerging reports that link the gut microbiota to brain function, it seems possible that maternal obesity-induced changes in the gut microbiome may be associated with cognitive impairments in the offspring.

Dietary fiber has been widely reported to regulate the gut microbiome, providing an essential substrate to the community of microbes that inhabits the distal gut (Sonnenburg and Sonnenburg, 2014). Unlike humans, who only produce around 17 gastrointestinal enzymes to digest food glycans, the gut microbiota produces thousands of complementary enzymes with diverse specificities, which enable them to depolymerize and ferment dietary polysaccharides into host-absorbable short-chain fatty acids (SCFAs) (El Kaoutari et al., 2013). SCFAs have various effects on the host brain. For example, acetate crosses the blood-brain barrier and regulates the activity of hypothalamic orexigenic neurons (Frost et al., 2014). Notably, SCFAs are vital molecules that modulate microglia maturation, morphology, and function (Erny et al., 2015). Additional evidence suggests that

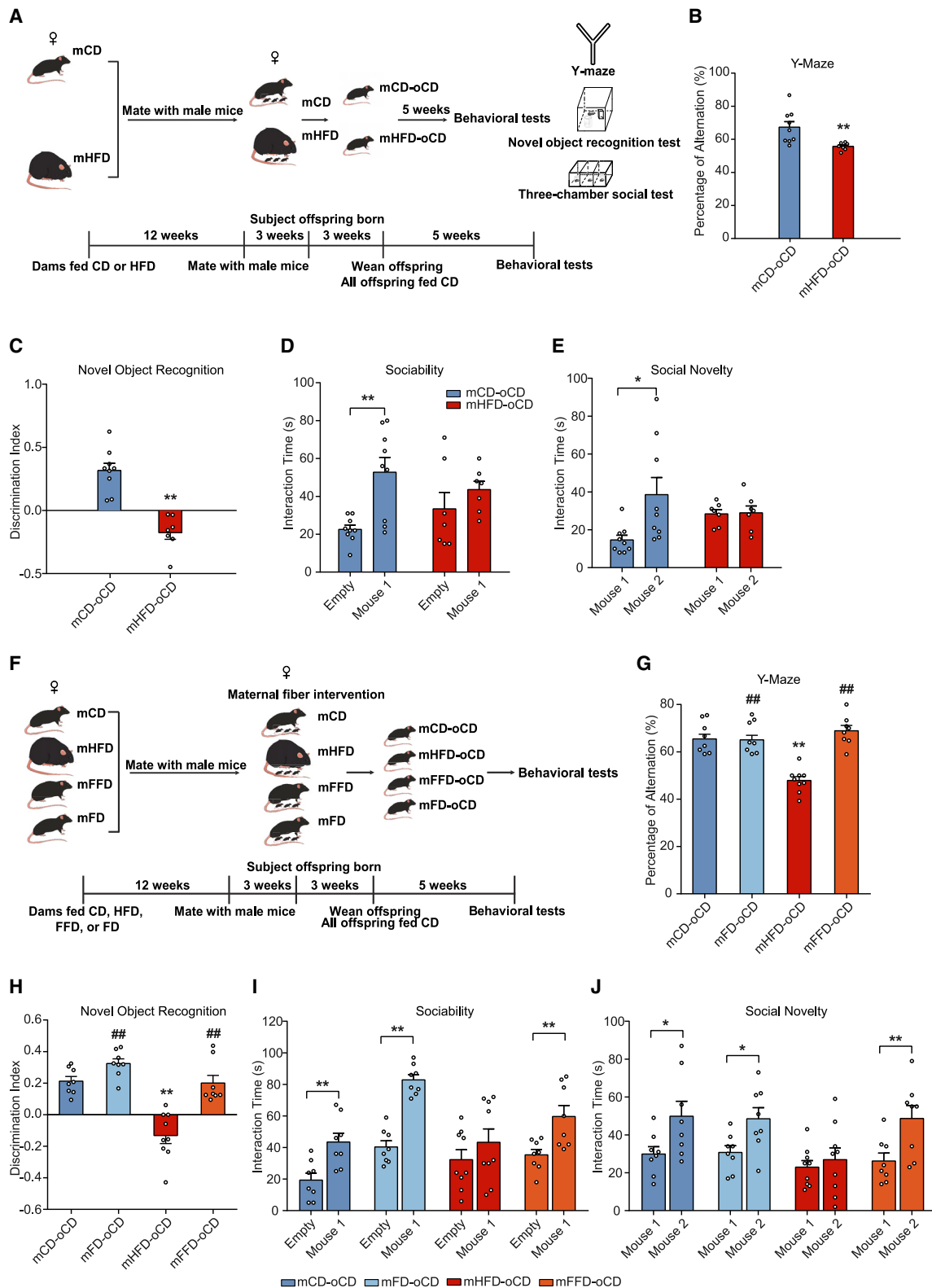


Figure 1. Maternal obesity and dietary fiber intake impact the cognitive and social behaviors of mouse offspring

(A) Schematic of the maternal diet regimen and breeding.

(B) For the Y-maze, spontaneous alternations were recorded.

(C) For the novel object recognition test, the discrimination index between the novel and familiar object was calculated.

(legend continued on next page)

dietary manipulation of the maternal microbiome in pregnancy with fiber has beneficial effects on the offspring's immune function and metabolism (Kimura et al., 2020; Thorburn et al., 2014). However, it remains unknown whether dietary fiber restores cognitive and social behavioral deficits in offspring of mothers with obesity.

This work was aimed to investigate the mechanistic connections between maternal obesity and cognitive behavioral deficits of offspring, as well as the beneficial effects of dietary fiber on the behavioral deficits of offspring. Here, we report that (1) maternal obesity induces cognitive and social behavioral deficits in human and mouse offspring; (2) maternal high-fiber intake improves offspring's social, behavioral deficits by restructuring the gut microbiome; (3) mother-to-offspring transmission of the gut microbiome mediates mHFD-induced learning and memory impairments in offspring; (4) offspring high-fiber intake improves gut microbiome and aberrant spliceosome alterations and restores mHFD-induced cognitive and social behavioral deficits in offspring; and (5) oral treatment with a mixture of acetate and propionate reverses mHFD-induced behavioral deficits in offspring.

RESULTS

Maternal pre-pregnancy overweightness and obesity are associated with impaired child neurodevelopment

To examine the association between maternal pregnancy weight and neurodevelopment in offspring, 778 children (403 boys and 375 girls) were eligible for follow-up. Children were aged 7–14 years and their parents completed the social competence scale of the child behavior checklist, which included 20 social competence items; these were divided into three social competence subscales that measured the following competencies: activities (e.g., sports and hobbies), social subjects (e.g., friendships and interpersonal skills), and school performance (e.g., learning ability). Demographics of the study population are shown in Table 1. Compared with normal-weight mothers, overweight and obese mothers had a significantly higher proportion of overweight and obese children ($p < 0.05$). Additionally, on average, overweight and obese mothers had lower educational attainment and lower family income than normal-weight mothers ($p < 0.001$). Linear regression analysis revealed that children of mothers with pre-pregnancy overweightness and obesity scored lower in social competence than children of mothers with a pre-pregnancy normal weight status after covariate adjustment (95% confidence interval [CI]: -1.89 to -0.02) (Table 1; Figure S1A). Consistent with cohort studies in other countries that found poorer cognitive performance and an increased risk of ASD in

children of mothers with obesity, the children of Chinese mothers who were overweight or obese had significantly reduced scores of social subjects and school performance, which indicates that they experienced a lower social and learning ability ($p < 0.05$; Table 1; Figures S1B–S1D). It has also been revealed that the significantly reduced social competence was more pronounced in boys than in girls, which could be associated with lower school performance scores ($p < 0.01$; Figures S1A–S1C). These data indicate that maternal obesity is more likely to be associated with cognitive and social impairments in male offspring than in female offspring.

Maternal obesity induces cognitive and social behavioral deficits in mouse offspring

In human studies, it is challenging to confirm causation or identify the mechanisms linking maternal obesity with offspring neurodevelopment. To investigate how maternal obesity affects offspring neurodevelopment, we established an animal model: female C57BL/6J mice were fed either a control diet (mCD) or a high-fat diet (mHFD) for 12 weeks. As expected, an mHFD significantly increased maternal weight ($p < 0.01$; Figure S2A). Female mice were then paired with male mice to produce offspring, which were then fed with a control diet (oCD) after weaning (3 weeks) (Figure 1A). There was no significant difference in offspring weight between the maternal diet groups at 8–10 weeks old (Figure S2B), when the behavioral experiments were performed. There were no differences in behavioral results between male and female offspring. To assess working memory and long-term memory, the Y-maze test and the novel object recognition test were performed, respectively. Compared with the mCD-oCD offspring, mHFD-oCD offspring had fewer spontaneous alternations and showed a discrimination index between the novel and familiar object close to -0.2 , which is indicative of working memory and long-term memory impairments ($p < 0.01$; Figures 1B, 1C, S2C, and S2D). Consistent with a previous report (Buffington et al., 2016), mHFD-oCD offspring had impaired sociability and showed no preference for social novelty in the three-chamber sociability test (Figures 1D, 1E, S2E, and S2F). These data indicate that maternal obesity led to memory and social deficits in offspring.

High-fiber intake in maternal diet restores maternal obesity-induced cognitive and social deficits in offspring

To investigate whether dietary fiber alleviates maternal obesity-induced neurodevelopment dysfunction in offspring, the pre-pregnancy female mice were fed with one of the four following diets: control diet (mCD), high-fat diet (mHFD),

(D) In the sociability test, the time spent interacting with a mouse or with an empty wire cage was recorded.

(E) In the social novelty test, the time spent interacting with a novel versus a familiar mouse was recorded.

(F) Schematic of the maternal dietary fiber supplementation.

(G–J) Behavioral phenotypes in offspring after maternal dietary fiber supplementation, including (G) Y-maze, (H) the novel object recognition test, (I) sociability, and (J) preference for social novelty.

Data are presented as the mean \pm SEM. (B–E) mCD-oCD, $n = 9$ mice, 5 litters; mHFD-oCD, $n = 7$ mice, 5 litters. (G–J) mCD-oCD, $n = 8$ mice, 6 litters; mFD-oCD, $n = 8$ mice, 5 litters; mHFD-oCD, $n = 9$ mice, 7 litters; mFFD-oCD, $n = 8$ mice, 7 litters. Statistical analyses were performed using unpaired two-tailed Student's t tests (B and C), paired two-tailed Student's t tests (D, E, I, and J), or a one-way ANOVA with Tukey's multiple comparison test (G and H). For Tukey's multiple comparison test, * $p < 0.05$, ** $p < 0.01$, compared with the mCD-oCD group; # $p < 0.05$, ## $p < 0.01$, compared with the mHFD-oCD group. For the Student's t test, * $p < 0.05$, ** $p < 0.01$. See also Figure S2.

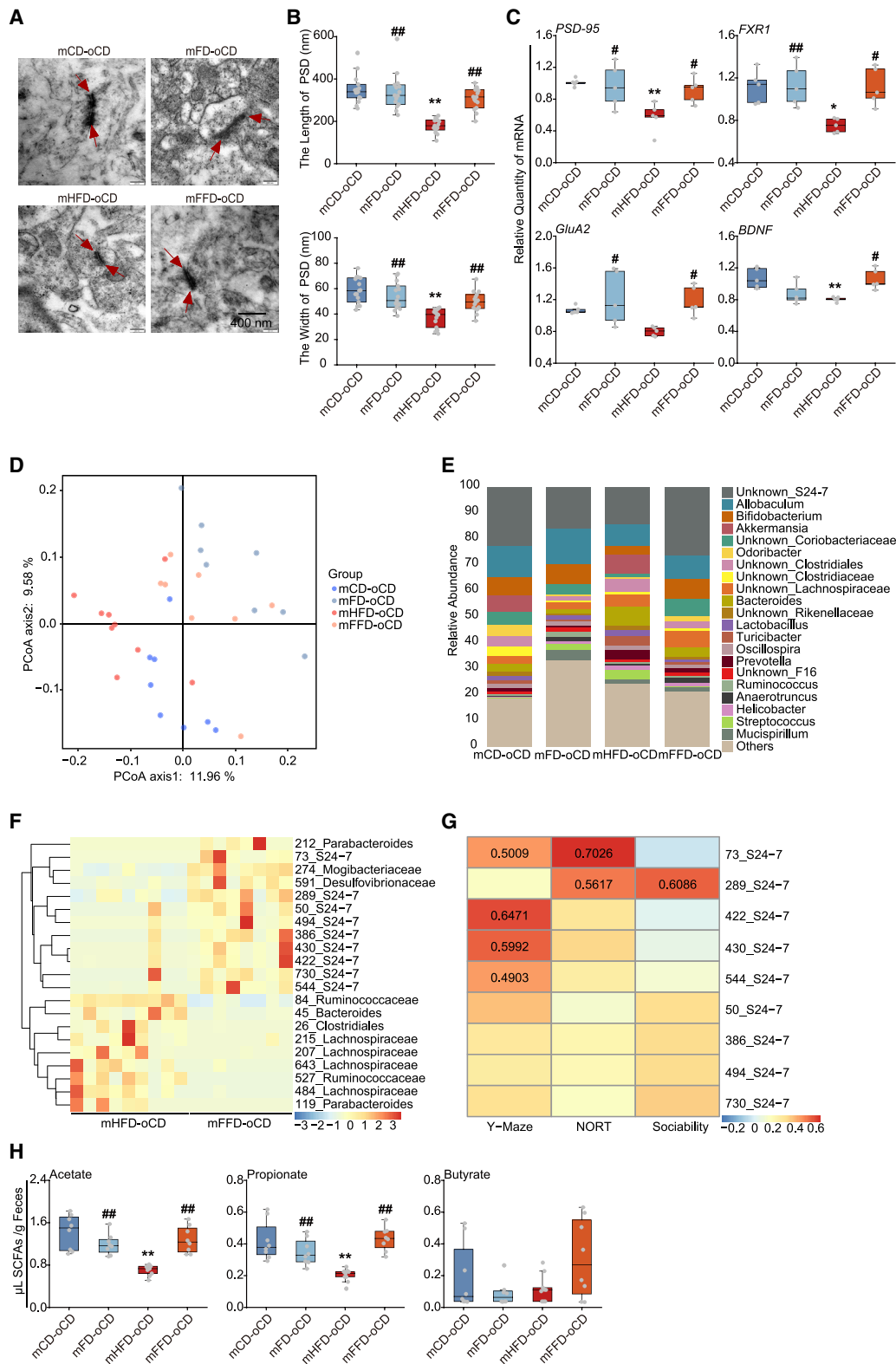


Figure 2. High-fiber intake in maternal diet restores synaptic impairments and re-shapes the gut microbiome of offspring

(A) Representative images of synapse ultrastructure.

(B) The length (up) and width of PSD (down) (n = 15 slices from 3 mice, 3 litters/group).

(C) The mRNA expressions of *PSD-95*, *FXR1*, *GluA2*, and *BDNF* in the hippocampus (n = 5 mice, 5 litters/group).

(legend continued on next page)

high-fat/high-fiber diet (a high-fat diet with inulin as a source of fiber, mFFD), and a control diet with inulin (mFD) for 12 weeks. Female mice were then paired with male mice to produce offspring that were fed with the control diet after weaning (Figure 1F). Consistent with reports of lower fertility in mothers with obesity (Poston et al., 2016), the litter size was reduced ($p < 0.01$; Figure S2I), and latency to first litter increased in female mice fed with an mHFD ($p < 0.01$; Figure S2J). Compared with the mHFD, high-fiber feeding reduced weight gain and markedly increased fertility ($p < 0.01$; Figures S2G–S2J). There was no significant difference in offspring weight between maternal diet cohorts at 8–10 weeks old (Figure S2K). Fecal samples were collected, and behaviors in offspring were assessed when the mice were 8–10 weeks old. Strikingly, maternal dietary fiber intake significantly improved working and long-term memory in the offspring, as well as sociability and the preference for social novelty in mHFD-oCD offspring (Figures 1G–1J and S2L–S2U). These results indicate that maternal dietary fiber intake protected against maternal obesity-induced cognitive and social behavioral deficits in offspring.

High-fiber intake in maternal diet restores maternal obesity-induced synaptic impairments in offspring

The ultrastructure of synapses in the hippocampus was examined. An analysis of postsynaptic density (PSD) revealed that the length and width of PSD were significantly elevated in the mFFD-oCD group compared with the mHFD-oCD group ($p < 0.01$; Figures 2A and 2B). Additionally, maternal obesity lowered the expressions of synaptic-plasticity-related genes (*PSD-95* and *FXR1*), neuronal development-related genes (*FXR2* and *TDP2*), NMDA receptor *GluN2B*, and AMPA receptor *GluA2* in the hippocampus and prefrontal cortex (PFC) of the offspring brain ($p < 0.05$), which were significantly restored by the high-fiber diet feeding ($p < 0.05$; Figures 2C, S3C, and S3E). Consistently, the protein level of PSD-95 was also restored in mFFD-oCD offspring compared with mHFD-oCD offspring, as assessed by immunofluorescence ($p < 0.01$; Figures S3A and S3D).

Given that microglia dysregulation has been reported in a range of neuropsychiatric conditions, including Alzheimer's disease and ASD (Frick et al., 2013; Salter and Stevens, 2017), we assessed the expression levels of microglia maturation-related genes (*MAFB*, *CD31*, *F4/80*, and *CSF1R*), microglia-neuron interaction-related genes (*BDNF*, *NGF*, *DAP12*, *CX3CR1*, and *CX3CL1*), microglia activation-related genes (*GSK3B* and *FYB*), and neuroinflammatory cytokines genes (*IL-1 β* and *TNF- α*) in the hippocampus and PFC. Maternal obesity lowered *MAFB*,

BDNF, *NGF*, *DAP12*, and *CX3CL1* but increased *CD31* and *F4/80* mRNA levels in offspring ($p < 0.05$), which were significantly restored by the high-fiber diet feeding ($p < 0.05$; Figures S3B, S3C, and S3E).

These findings are consistent with reports of shared mechanisms underlying social and cognitive impairments (State, 2010). These results indicate that maternal high-fiber intake protects offspring against synaptic impairment and disruption of microglia maturation in the hippocampus and PFC, which were induced by maternal obesity.

High-fiber intake in maternal diet re-shapes the gut microbiome in both mother and offspring mice

Maternal obesity has been shown to alter the offspring's gut microbiome (Chu et al., 2016), and microbial reconstitution has been reported to reverse social deficits (Buffington et al., 2016). Dietary fiber is a well-recognized prebiotic known to promote the proliferation of beneficial bacteria in the colon (Gibson, 1999). Hence, we next examined whether dietary fiber protection against mHFD-induced behavioral deficits was correlated with microbiota alterations. Analysis of microbiota composition by 16S sequencing indicated that there was a change in the maternal microbiome composition, but not community richness, between the mHFD group and the mFFD group (Figures S4A and S4B). Maternal dietary fiber intake also corrected some of the mHFD-induced changes in the microbiota observed at the phylum level and order level (Figures S4C and S4D; Table S1). Specifically, S24-7, *Bifidobacterium animalis*, *Prevotella*, and Clostridiales were prevalent in most mFFD samples and absent from most or all mHFD samples (Figure S4E).

While bacterial α -diversity did not differ between the offspring from any diet group (Figure S4F), the unweighted UniFrac distance of the mFFD-oCD mice was different from mHFD-oCD mice, similarly to that observed in their dams, which revealed that the dietary fiber regimen altered the microbiota composition (Figures 2D and S4A). Differentiating bacterial taxa in offspring belonged predominantly to the Clostridiales and Bacteroidales orders, with single representatives from the Actinobacteria, Firmicutes, and Tenericutes phyla (Figures 2E, S4G, and S4H). Specifically, 21 differentiating bacterial taxa were identified between mHFD-oCD and mFFD-oCD groups, using the Wilcoxon rank-sum test to analyze operational taxonomic units (OTUs), nine of which belonged to the S24-7 family (Figure 2F). The abundance of five bacterial OTUs were positively correlated with increased cognitive and social behaviors in mice, as assessed using Spearman's rank correlation ($r > 0.4$, $p < 0.05$; Figure 2G). The association of specific bacterial species with mFFD-oCD

(D) Principal coordinates analysis (PCoA) of unweighted UniFrac distances from the averaged rarefied 16S rRNA gene dataset ($p = 0.0001$, $R^2 = 0.1993$).

(E) The relative abundance of bacteria at the genus level. All genera with an average relative abundance below 1% were grouped to "others."

(F) A Z score-scaled heatmap of different OTUs identified using the Wilcoxon rank-sum test between mHFD-oCD and mFFD-oCD, with $p \leq 0.01$.

(G) The abundance of select taxa in the offspring microbiome was correlated with the behavior of offspring. Spearman's rank correlation was performed to assess the correlation between the microbiome and mouse behavior. If $p < 0.05$ for significant correlations, then the r value is noted. NORT, novel object recognition test.

(H) The concentrations of SCFAs, including acetate, propionate, and butyrate, in offspring feces.

Data in (B), (C), and (H) are presented as the median \pm interquartile range. (D–H) mCD-oCD, $n = 8$ mice, 6 litters; mFD-oCD, $n = 8$ mice, 5 litters; mHFD-oCD, $n = 9$ mice, 7 litters; mFFD-oCD, $n = 8$ mice, 7 litters. Statistical analyses were performed using a one-way ANOVA with Tukey's multiple comparison test (B, C, and H). * $p < 0.05$, ** $p < 0.01$, compared with the mCD-oCD group; # $p < 0.05$, ## $p < 0.01$, compared with the mHFD-oCD group. The gut microbiome of mHFD-oCD and mCD-oCD group in Figures 2, 5, S4, and S6 are from same mouse fecal samples. See also Figures S3 and S4.

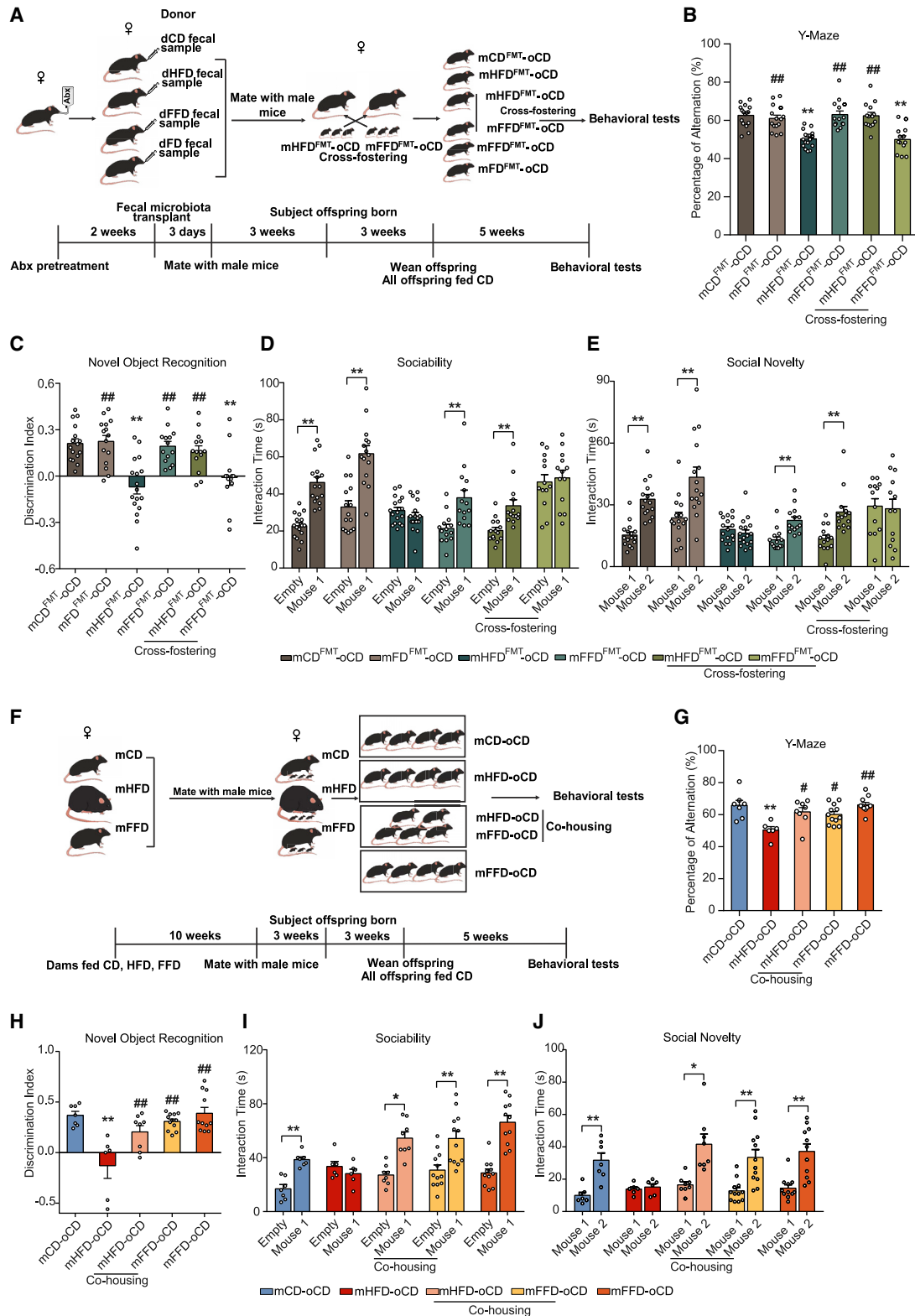


Figure 3. Gut microbiota mediates maternal obesity-induced cognitive and social deficits in offspring

(A) Schematic of the maternal fecal microbiota transplant and cross-fostering experiments.

(B–E) The offspring from fecal microbiota-transplanted mothers were tested using (B) the Y-maze, (C) the novel object recognition test, (D) sociability, and (E) preference for social novelty.

(legend continued on next page)

samples, which were also positively correlated with increased cognitive- or social-relevant behaviors, supports the hypothesis that particular bacteria may contribute to the protective effect of dietary fiber against mHFD-induced cognitive and social deficits in offspring.

Microbial metabolites in the gut are thought to impact neurological outcomes (Wang et al., 2018). We examined SCFAs in offspring feces, which are derived from the microbial fermentation of dietary fibers and are likely to have broad impacts on various aspects of host physiology. Dietary fiber treatment improved mHFD-induced decreases in feces levels of acetate and propionate, but not butyrate, in offspring ($p < 0.01$; Figure 2H). Additionally, we found that the expression levels of the SCFA receptor, *Olfir78*, was significantly lower in the hippocampus and PFC of the mHFD-oCD offspring than in the control group ($p < 0.05$; Figure S4I). However, the high-fiber diet significantly increased the expression of *Olfir78* in the hippocampus and PFC ($p < 0.05$; Figure S4I).

Gut microbiota mediates maternal obesity-induced cognitive and social deficits in offspring

The maternal gut microbiome can be vertically transmitted to their offspring, which leads to longer-lasting colonization of the offspring gut (Ferretti et al., 2018; Yassour et al., 2018). To investigate whether the gut microbiota plays a vital role in mHFD-induced behavioral abnormalities, the fecal microbiota from female donor mice (dCD, dFD, dHFD, and dFFD) were transplanted into antibiotic-treated adult female mice (rCD, rFD, rHFD, and rFFD) (Figures 3A, S5A, and S5B). Offspring from rHFD dams showed impaired memory and social behaviors (Figures 3B–3E and S5C–S5I). By contrast, offspring from the rFFD dams had no behavioral abnormalities (Figures 3B–3E and S5C–S5I).

Subsequently, to investigate whether maternal colonization of microbiota influence behaviors in offspring after birth, cross-fostering experiments were performed by switching newborns from rHFD and rFFD dams. Strikingly, offspring of rHFD dams, reared by rFFD dams, exhibited behavioral improvements; offspring of rFFD mothers, reared by rHFD fecal microbiota-transplanted mothers, exhibited behavioral impairments (Figures 3A–3E and S5C–S5I). Accordingly, mHFD-oCD offspring were co-housed with mFFD-oCD offspring, thus allowing the transfer of microbiota via coprophagy (Figures 3F and S5J). mHFD-oCD offspring co-housed with mFFD-oCD offspring exhibited an increased cognition, as well as improved sociability and a greater preference for social novelty, as determined by behavioral tests (Figures 3G–3J and S5K–S5Q). These results indicate that there is a causal relationship between gut microbiota disturbances and behavioral deficits in the offspring of mice with maternal obesity, and that maternal dietary fiber intake could

protect against behavioral deficits of offspring via regulation of the gut microbiota.

High-fiber intake in offspring's diet restores maternal obesity-induced behavioral deficits and aberrant spliceosome alterations

We next examined whether direct dietary fiber application to offspring could also reverse the behavioral and neurobiological deficits that were characteristic of mHFD-oCD offspring. Offspring from obese dams were fed a control diet with inulin (mHFD-oFD) from weaning (3 weeks) until adulthood, after which behavioral testing began (Figures 4A, S6A, and S6B). Treatment with dietary fiber significantly improved cognition, as well as sociability and the preference for social novelty (Figures 4B–4E and S6C–S6I).

Gene expression profiling of RNA-seq identified 564 downregulated and 247 upregulated genes in the hippocampus of mHFD-oFD and mCD-oFD mice, using differentially expressed gene (DEG) analysis (FDR $q < 5\%$) (Figure S6J). There were relatively few sex-specific DEGs (Figure S6K). Gene set enrichment analysis (GSEA) indicated that KEGG pathways involving transcription, translation, and protein quality control and export were upregulated in the hippocampus of the mHFD-oCD group mice compared with the mHFD-oFD group mice (Figure 4F). A KEGG pathway involving RNA processing by the spliceosome was significantly upregulated in mHFD-oCD mice (FDR $q < 25\%$) (Figures 4G and 4H). These data revealed that direct dietary fiber administration to 3-week-old offspring also effectively improved behavior and RNA splicing processes.

High-fiber intake in offspring's diet re-shapes the gut microbiome

As shown in Figures 5A and S6L, the high-fiber diet feeding in the offspring significantly reshaped the gut microbiome. Differentiating bacterial taxa belonged predominantly to the Clostridiales and Bacteroidales orders, with single representatives from the Firmicutes phyla (Figures 5B, S6M, and S6N). Consistent with the maternal dietary fiber supplement, the high-fiber diet feeding in the offspring increased the level of S24-7 (Figure 5C). Specifically, *Bacteroides* were prevalent in all mHFD-oFD samples and absent from most or all mHFD-oCD samples (Figure 5C). Conversely, *Ruminococcus* was prevalent among most mHFD-oCD mice and absent from the mHFD-oFD group (Figure 5C). The abundance of the eight OTUs belonging to S24-7 was positively correlated with long-term memory ($r > 0.4$, $p < 0.05$; Figure 5D). Additionally, the level of *Bacteroides* was significantly positively correlated with long-term memory and social behaviors ($r > 0.5$, $p < 0.05$; Figure 5D). *Ruminococcus* showed opposite effects, and its levels were correlated with reduced memory

(F) Schematic of the offspring co-housing experiment.

(G–J) The co-housed offspring were tested using (G) the Y-maze, (H) the novel object recognition test, (I) sociability, and (J) preference for social novelty. Data are presented as the mean \pm SEM. (B–E) mCD^{FMT}-oCD, $n = 16$ mice, 7 litters; mFD^{FMT}-oCD, $n = 15$ mice, 5 litters; mHFD^{FMT}-oCD, $n = 17$ mice, 5 litters; mHFD^{FMT}-oCD (cross-fostering), $n = 14$ mice, 3 litters; mFFD^{FMT}-oCD (cross-fostering), $n = 13$ mice, 3 litters; mFFD-oCD, $n = 14$ mice, 4 litters. (G–J) mCD-oCD, $n = 7$ mice, 3 litters; mHFD-oCD, $n = 6$ mice, 6 litters; mHFD-oCD (co-housing), $n = 8$ mice, 4 litters; mFFD-oCD (co-housing), $n = 12$ mice, 6 litters; mFFD-oCD, $n = 11$ mice, 5 litters. Statistical analyses were performed using a one-way ANOVA with Tukey's multiple comparison test (B, C, G, and H) or using paired two-tailed Student's *t* tests (D, E, I, and J). For (B) and (C), * $p < 0.05$, ** $p < 0.01$, compared with the mCD^{FMT}-oCD group; # $p < 0.05$, ## $p < 0.01$, compared with the mHFD^{FMT}-oCD group. For (G) and (H), * $p < 0.05$, ** $p < 0.01$, compared with the mCD-oCD group; # $p < 0.05$, ## $p < 0.01$, compared with the mHFD-oCD group. For the Student's *t* test, * $p < 0.05$, ** $p < 0.01$. See also Figure S5.

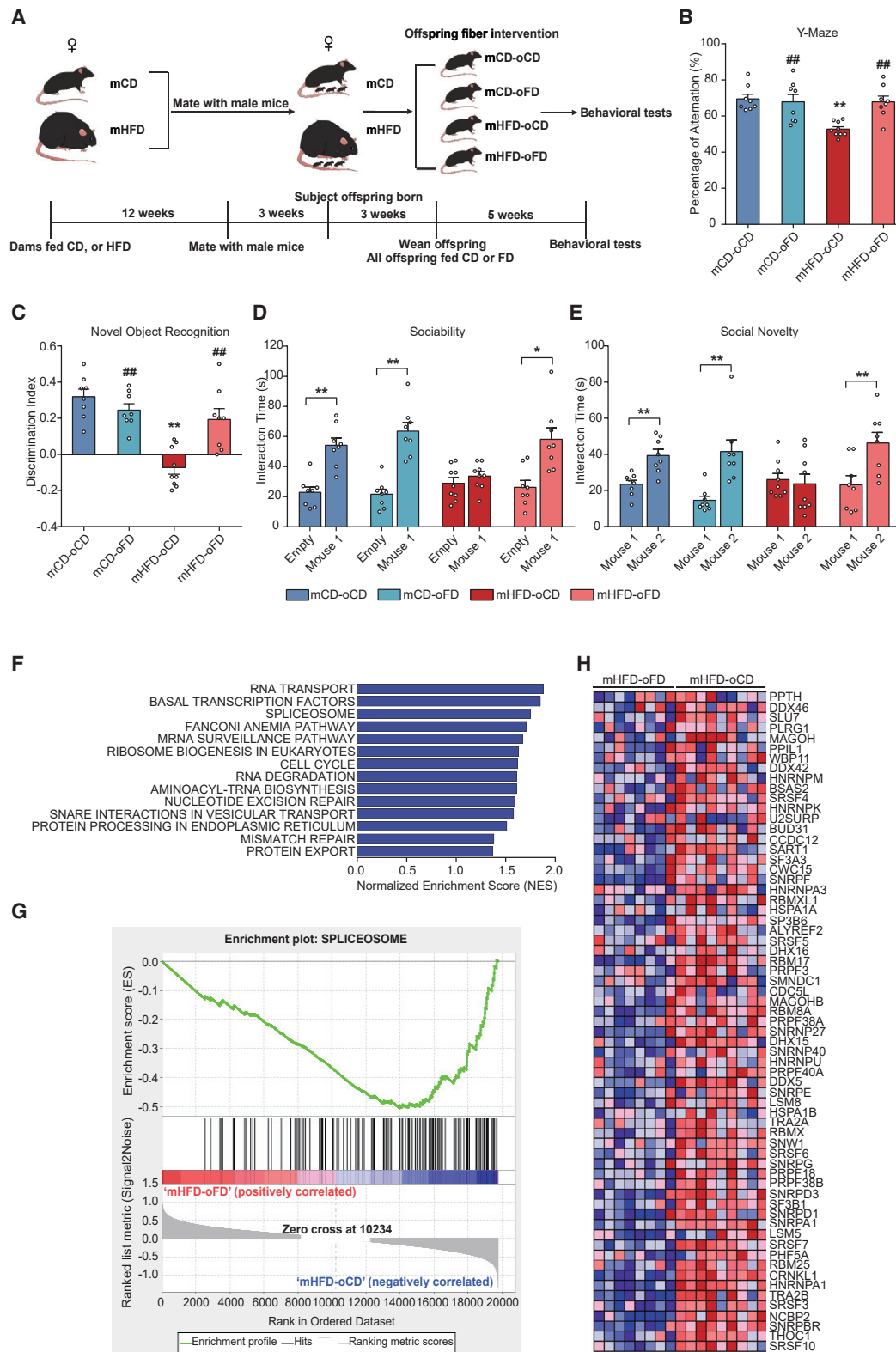


Figure 4. High-fiber intake in offspring's diet restores maternal obesity-induced behavioral deficits and aberrant spliceosome alterations
(A) Schematic of the direct dietary fiber administration to offspring.
(B–E) Behavioral phenotypes in offspring after dietary fiber administration, including (B) the Y-maze, (C) the novel object recognition test, (D) sociability, and (E) preference for social novelty

behavior and social interaction deficits ($r > 0.5$, $p < 0.05$; [Figure 5D](#)). These findings suggest that offspring dietary fiber intake could also correct the microbiota depletion in offspring born to mothers with obesity.

SCFAs restore maternal obesity-induced cognitive and social behavioral deficits in offspring

In accordance with the maternal dietary fiber supplement, dietary fiber treatment elevated levels of SCFAs in mHFD-oFD offspring ([Figure 5E](#)). Furthermore, the level of acetate and propionate were significantly correlated with the most differentiating bacterial taxa ($r > 0.4$, $p < 0.05$; [Figure 5F](#)). We hypothesized that the selective decrease of acetate and propionate in the gut of mHFD-oCD offspring was causally related to their behavioral deficits. To determine this hypothesis, acetate and propionate were supplemented into the drinking water of offspring born to obese dams at weaning for 5 weeks, after which behaviors were tested ([Figures 6A and S7A](#)). SCFA supplementation significantly improved the serum levels of acetate, but not propionate in offspring ($p < 0.05$; [Figure S7B](#)). Remarkably, treatment with a mix of acetate and propionate significantly improved cognition, as well as sociability and preference for social novelty of offspring ([Figures 6B–6E and S7C–S7I](#)). SCFA supplementation significantly increased the expression of *Olfir78* in the hippocampus and PFC ($p < 0.05$; [Figure S7J](#)). Accordingly, SCFA treatment significantly improved the length and width of the PSD ($p < 0.01$; [Figures 6F and 6G](#)). SCFAs also promoted microglial maturation, microglia-neuron interaction, and synaptic function in the hippocampus and PFC of offspring by increasing the expressions of *MAFB*, *NGF*, *PSD-95*, *GluN2B*, and *GluA2* and reducing the expression of *CD31* in the hippocampus and PFC ([Figures S7K and S7L](#)). These observations highlight the importance of SCFAs, which rendered offspring resistant to social and cognitive impairments.

DISCUSSION

In this study, we found that maternal pre-pregnancy overweightness and obesity are strongly associated with a poorer cognitive performance and sociality of their children. Consistent with this, maternal obesity also induced cognitive and social behavioral deficits in the offspring of a mouse model. Furthermore, high-fiber intake in the diet of either the dam or its offspring improved the behavioral deficits, synaptic damage, and aberrant spliceosome alterations in the offspring. Colonization of the gut microbiota from obese donors in the dams led to cognitive and social behavioral disorders in offspring. However, transplantation of the gut microbiota from high-fiber intake donors resulted in a better behavioral performance. These results indicate that there is a causal relationship between a maternal gut microbiota composition disturbance and behavioral changes in offspring, which was further confirmed by the cross-fostering experiment. Notably,

the co-housing experiment revealed that manipulating the offspring's gut microbiome community after weaning could also reduce the maternal obesity-induced behavioral deficits. Moreover, SCFA treatment in the offspring after weaning attenuated the maternal obesity-induced cognitive and social impairments. These results further suggest that a high-fiber diet can protect against the behavioral deficits of offspring, possibly by restructuring the gut microbiome and enhancing the formation of microbial metabolites.

Recent studies have also reported that dietary fibers can improve cognitive performance and anxiety and depression in rodent models ([Burokas et al., 2017](#); [Messaoudi et al., 2005](#)). In this study, high-fiber intake alleviated the working and long-term memory impairments of the offspring of high-fat-diet-fed dams, which, to the best of our knowledge, has not been reported before. Notably, maternal dietary fiber intake could also restore social behavior abnormalities, as well as the preference for social novelty, in both male and female offspring. Similarly, high-fiber intake in offspring's diet also mitigated the maternal obesity-induced cognitive and social deficits. RNA-seq analysis of the offspring's hippocampi indicated that several disease-related pathways were regulated by high-fiber intake. Notably, offspring dietary fiber intake significantly reversed the upregulation of the KEGG pathway of the spliceosome (mmu03040) in the hippocampi. Recent studies have highlighted the importance of aberrant alternative splicing of mRNA in the brains of subjects with an ASD diagnosis ([Gandal et al., 2018](#); [Gonatopoulos-Pournatzis et al., 2018](#)). These experimental findings indicate that high dietary fiber intake could be an effective intervention to mitigate the influence of maternal obesity on the development of offspring's central nervous system.

The broad impacts of dietary fibers on various aspects of host physiology occur via adjustment of the gut microbiota diversity. Here, we found that high-fiber intake in the maternal diet markedly altered the gut microbiota in the offspring of obese dams. Notably, OTUs belonging to S24-7 were found to be positively correlated with cognitive and social behaviors in mice. However, to the best of our knowledge, the S24-7 family microbe species are not fully understood, as the family classification is still ambiguous ([Ormerod et al., 2016](#)). However, a recent study reported that microbes from the S24-7 family were strongly associated with complex carbohydrate degradation in the gut ([Lagkouvardos et al., 2019](#)). Interestingly, [Park et al. \(2017\)](#) reported that the abundance of unclassified members of S24-7 was significantly decreased in a mouse model of Alzheimer's disease. Moreover, high-fiber intake in the offspring diet lowered the relative abundance of *Ruminococcus* and increased the *Bacteroides*. Thus, the influence of a high-fiber intake in the offspring's diet on the gut microbiota composition was different from the maternal intervention, which could be a result of the combined effects of mother-to-infant microbial transmission and shared environmental factors.

(F) KEGG pathways upregulated in the hippocampus of mHFD-oCD mice by GSEA (FDR < 25%).

(G and H) The enrichment plot (G) and heatmap of the leading-edge subset (H) for the spliceosome set.

Data in (B)–(E) are presented as the mean \pm SEM. (B–H) mCD-oCD, $n = 8$ mice, 5 litters; mCD-oFD, $n = 8$ mice, 4 litters; mHFD-oCD, $n = 9$ mice, 5 litters; mHFD-oFD, $n = 8$ mice, 5 litters. Statistical analyses were performed using a one-way ANOVA with Tukey's multiple comparison test (B and C) or using paired two-tailed Student's t tests (D and E). For Tukey's multiple comparison test, * $p < 0.05$, ** $p < 0.01$, compared with the mCD-oCD group; # $p < 0.05$, ## $p < 0.01$, compared with the mHFD-oCD group. For the Student's t test, * $p < 0.05$, ** $p < 0.01$. See also [Figure S6](#).

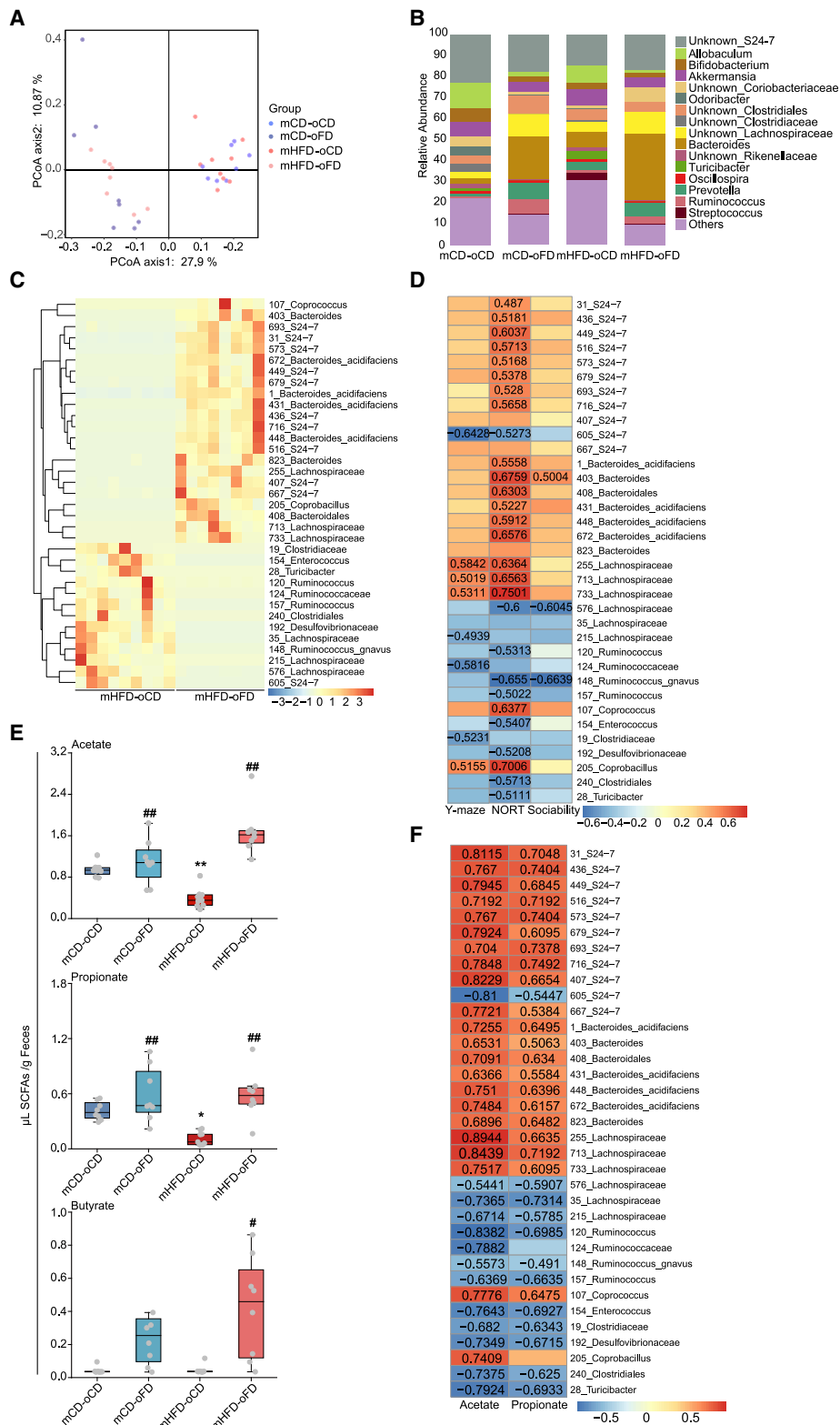


Figure 5. High-fiber intake in offspring's diet re-shapes the gut microbiome

(A) Principal coordinates analysis (PCoA) of unweighted UniFrac distances from the averaged rarefied 16S rRNA gene dataset ($p = 0.0001$, $R^2 = 0.3395$).
 (B) The relative abundance of bacteria at the genus level. All genera with an average relative abundance below 1% were grouped to "others."
 (C) A Z score-scaled heatmap of different OTUs identified by the Wilcoxon rank-sum test between mHFD-oCD and mHFD-oFD with $p \leq 0.001$.

(legend continued on next page)

One possible explanation of how gut bacteria can affect gene expression and host behaviors is by their generation of various metabolites (Hsiao et al., 2013). SCFAs, including acetate and propionate, have been reported to be the key molecules that modulate microglia maturation, morphology, and function; thus, they could affect CNS function (Erny et al., 2015). Previous studies have reported that neurodevelopmental abnormalities in people with ASD are accompanied by impaired acetate and propionic acid metabolism (Liu et al., 2019; Wang et al., 2020). Similarly, we found that the concentrations of acetate and propionate in feces were reduced in the offspring of obese dams. However, the formation of these SCFAs was restored by maternal or offspring dietary fiber intake, accompanied by behavioral improvements. Furthermore, SCFA treatment significantly attenuated the maternal obesity-induced cognitive and social impairments in the offspring. However, the precise mechanism by which SCFAs rescue social and cognitive behaviors remains to be determined. It has been widely reported that the gut microbiota and SCFAs play roles in mediating microglial maturation and function in the brain (Erny et al., 2015). Consistent with these reports, we found that SCFAs might also protect the synaptic structure by balancing the expression of microglia homeostasis- and function-related genes. Previous studies have indicated that the expression of pro-inflammatory cytokines is increased in the brains of offspring born to obese mothers (Bilbo and Tsang, 2010; Kang et al., 2014). However, we did not observe any neuroinflammatory responses in the mHFD-oCD or mFFD-oCD offspring.

Taken together, our results demonstrate that the cognitive and social dysfunctions associated with maternal obesity are induced by alterations of the intestinal microbiota of offspring. Furthermore, our findings indicate that maternal or offspring dietary fiber intake can reverse behavioral dysfunction by regulating the bacterial composition and SCFA formation. This work therefore provides new insights into the mechanism by which a marked shift in microbial ecology, caused by pre-pregnancy obesity, can negatively impact both cognitive and social behaviors in offspring. These results offer a more in-depth understanding of the causative link and underlying mechanisms of the effects of maternal obesity on offspring neurodevelopment in humans. Furthermore, we found that dietary fiber intervention for dams, or for 3-week-old offspring from obese mothers, could restore abnormal neurocognitive and social behaviors in the offspring, which suggests that behavioral abnormalities in children could be rectified during both prenatal brain development and postnatally. Overall, this finding opens up new research avenues into preemptive therapies for neurodevelopmental disorders that target the maternal and/or offspring gut microbiota and indicates that dietary fiber is a potential non-invasive, timely, and tractable treatment for neurodevelopmental disorders.

Limitations of study

Our study has some limitations that should be noted. First, our samples in the human study covered only two cities from eastern China. Thus, it is unclear how well the result generalizes to other populations. Further studies in regions are needed to verify our results. However, as our sample size is large, we believe that our results do represent reality. Second, it is unclear how nutrition status in the different stages of pregnancy and during lactation influence the gut microbiome and neurodevelopment of offspring. Another limitation is that we consider each offspring but not the litter as one unit in the statistical analysis. However, the analysis method was supported by numerous studies and limited animal use, considering animal welfare. Additionally, although we found that SCFA-mediated microglial maturation and function might play an essential role in regulating the neurodevelopment of offspring, the precise molecular mechanisms and signaling pathways involved remain to be determined. Future studies are also needed to evaluate synaptic plasticity, neuronal excitability in the hippocampus, PFC, amygdala, and other related brain regions in offspring.

STAR★METHODS

Detailed methods are provided in the online version of this paper and include the following:

- KEY RESOURCES TABLE
- RESOURCE AVAILABILITY
 - Lead contact
 - Materials availability
 - Data and code availability
- EXPERIMENTAL MODEL AND SUBJECT DETAILS
 - Human study
 - Animal study
 - Dietary fiber treatment
- METHOD DETAILS
 - Microbiota depletion
 - Gut microbiota transplantation
 - Cross-fostering
 - Co-housing
 - SCFAs treatment
 - Y-maze
 - Novel object recognition
 - Three-chamber social test
 - 16S rRNA microbiome sequencing
 - Fecal SCFAs assay
 - Serum SCFAs assay
 - RNA isolation and qRT-PCR
 - RNA sequencing analysis
 - Immunofluorescence

(D) The abundance of selected taxa in the offspring microbiome was correlated with the behavior of offspring, as tested using Spearman's rank correlation between the microbiome and mouse behaviors. If $p < 0.05$ for significant correlations, r is noted.

(E) SCFA concentrations in feces. Data are presented as the median \pm interquartile range.

(F) Spearman's rank correlation between the selected taxa of the microbiome and acetate/propionate. If $p < 0.05$ for significant correlations, r is noted.

(A–F) mCD-oCD, $n = 8$ mice, 5 litters; mCD-oFD, $n = 8$ mice, 4 litters; mHFD-oCD, $n = 9$ mice, 5 litters; mHFD-oFD, $n = 8$ mice, 5 litters. For (E), significant differences between the mean values were determined using a one-way ANOVA with Tukey's multiple comparison test. * $p < 0.05$, ** $p < 0.01$, compared with the mCD-oCD group; # $p < 0.05$, ## $p < 0.01$, compared with the mHFD-oCD group. The gut microbiome of mHFD-oCD and mCD-oCD group in Figures 2, 5, S4, and S6 are from same mouse fecal samples. See also Figure S6.

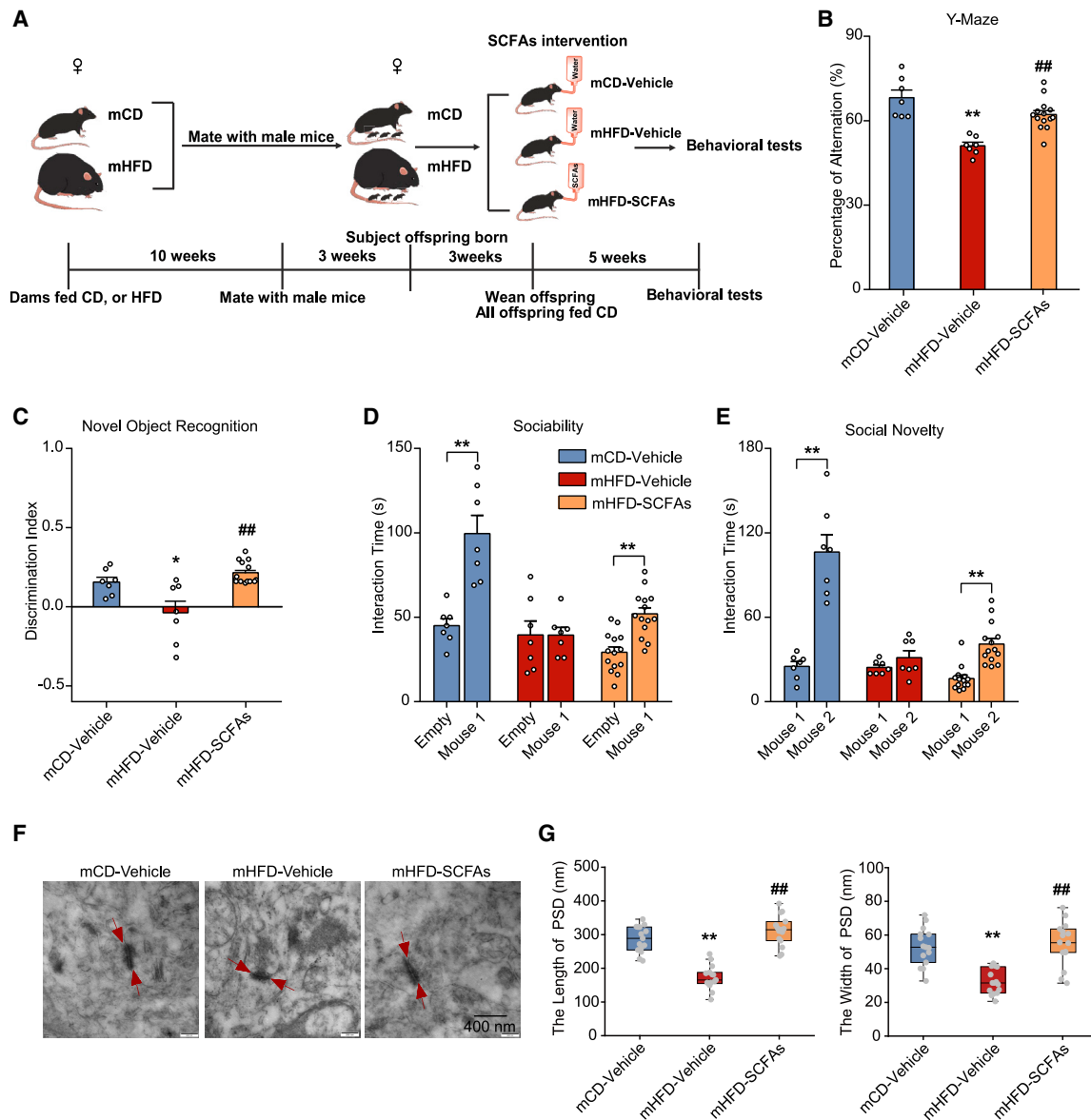


Figure 6. SCFAs restore maternal obesity-induced cognitive and social behavioral deficits in offspring

(A) Schematic of the treatment with a mixture of acetate and propionate.

(B–E) Behavioral phenotypes in the offspring after treatment with a mixture of acetate and propionate, including (B) the Y-maze, (C) the novel object recognition test, (D) sociability, and (E) preference for social novelty ($n = 7$ – 14 mice/group).

(F) Representative images of synapse ultrastructure.

(G) The length (left) and width (right) of the PSD ($n = 15$ slices from 3 mice, 3 litters /group).

Data presented in (B)–(E) are presented as the mean \pm SEM. Data in (G) are presented as the median \pm interquartile range. (B–E) mCD-vehicle, $n = 7$ mice, 4 litters; mHFD-vehicle, $n = 7$ mice, 4 litters; mHFD-SCFAs, $n = 14$ mice, 6 litters. Statistical analyses were performed using a one-way ANOVA with Tukey's multiple comparison test (B, C, and G) or using paired two-tailed Student's *t* tests (D and E). For Tukey's multiple comparison test, $*p < 0.05$, $**p < 0.01$, compared with the mCD-vehicle group; $\#p < 0.05$, $\#\#p < 0.01$, compared with the mHFD-vehicle group. For the Student's *t* tests, $*p < 0.05$, $**p < 0.01$. See also Figure S7.

○ Transmission electron microscopy

● QUANTIFICATION AND STATISTICAL ANALYSIS

SUPPLEMENTAL INFORMATION

Supplemental Information can be found online at <https://doi.org/10.1016/j.cmet.2021.02.002>.

ACKNOWLEDGMENTS

This work was financially supported by the National Key Research and Development Program of China (no. 2017YFD0400200), the National Natural Science Foundation of China (no. 81871118 and 81803231), the Innovative Talent Promotion Program-Technology Innovation Team (2019TD-006), the General Financial Grant from China Postdoctoral Science Foundation (no. 2016M602867), and the Special Financial Grant from China Postdoctoral

Science Foundation (no. 2018T111104). Z.L. is also funded by the Tang Cornell-China Scholars Program from Cornell University in the U.S. and the Alexander Von Humboldt-Stiftung in Germany. We also thank Zixin He, Han Li, Junhe Zhao, and Hang Zhao (Northwest A&F University, China) for their help during animal experiments.

AUTHOR CONTRIBUTIONS

Xiaoning Liu, X. Li, B.X., X.J., Q.Z., Z.Z., S. Yan, L.L., S. Yuan, S.Z., X.D., M.H., Z.L., and Xuebo Liu performed the experiments and analyzed the data; Xiaoning Liu, W.Z., F.Y., E.C., R.H.L., B.Z., M.H., Z.L., and Xuebo Liu wrote the manuscript; Xiaoning Liu, X. Li, X.J., Z.Z., S. Yan, M.H., Z.L., and Xuebo Liu prepared the figures; M.H., Z.L., and Xuebo Liu supervised the project. All authors read and approved the final manuscript.

DECLARATION OF INTERESTS

The authors declare no competing interests.

Received: August 5, 2020

Revised: December 8, 2020

Accepted: February 1, 2021

Published: March 1, 2021

SUPPORTING CITATIONS

The following references appear in the Supplemental Information: Adachi et al. (2018); Cook et al. (2014); Davies et al. (2008); Guo et al. (2015); Kaifu et al. (2003); Kratsman et al. (2016); Martin et al. (2017); Pluznick et al. (2013); Raverdeau et al. (2012); Rydbirk et al. (2016); Shimizu et al. (2017); Sunkaria et al. (2017); Walter and Crews (2017); Wang et al. (2019); Xiao et al. (2017); Zhang et al. (2020).

REFERENCES

Adachi, M., Mizuno-Kamiya, M., Takayama, E., Kawaki, H., Inagaki, T., Sumi, S., Motohashi, M., Muramatsu, Y., Sumitomo, S.-I., Shikimori, M., et al. (2018). Gene expression analyses associated with malignant phenotypes of metastatic sub-clones derived from a mouse oral squamous cell carcinoma Sq-1979 cell line. *Oncol. Lett.* **15**, 3350–3356.

Arai, K., Matsuki, N., Ikegaya, Y., and Nishiyama, N. (2001). Deterioration of spatial learning performances in lipopolysaccharide-treated mice. *Jpn. J. Pharmacol.* **87**, 195–201.

Basatemur, E., Gardiner, J., Williams, C., Melhuish, E., Barnes, J., and Sutcliffe, A. (2013). Maternal prepregnancy BMI and child cognition: a longitudinal cohort study. *Pediatrics* **131**, 56–63.

Batterham, R.L., Cowley, M.A., Small, C.J., Herzog, H., Cohen, M.A., Dakin, C.L., Wren, A.M., Brynes, A.E., Low, M.J., Ghatei, M.A., et al. (2002). Gut hormone PYY (3-36) physiologically inhibits food intake. *Nature* **418**, 650–654.

Bilbo, S.D., and Tsang, V. (2010). Enduring consequences of maternal obesity for brain inflammation and behavior of offspring. *FASEB J.* **24**, 2104–2115.

Buffington, S.A., Di Prisco, G.V., Auchtung, T.A., Ajami, N.J., Petrosino, J.F., and Costa-Mattoli, M. (2016). Microbial reconstitution reverses maternal diet-induced social and synaptic deficits in offspring. *Cell* **165**, 1762–1775.

Burokas, A., Arboleya, S., Moloney, R.D., Peterson, V.L., Murphy, K., Clarke, G., Stanton, C., Dinan, T.G., and Cryan, J.F. (2017). Targeting the microbiota-gut-brain axis: prebiotics have anxiolytic and antidepressant-like effects and reverse the impact of chronic stress in mice. *Biol. Psychiatry* **82**, 472–487.

Cho, I., and Blaser, M.J. (2012). The human microbiome: at the interface of health and disease. *Nat. Rev. Genet.* **13**, 260–270.

Chu, D.M., Antony, K.M., Ma, J., Prince, A.L., Showalter, L., Moller, M., and Aagaard, K.M. (2016). The early infant gut microbiome varies in association with a maternal high-fat diet. *Genome Med.* **8**, 77.

Cook, D., Nuro, E., Jones, E.V., Altamimi, H.F., Farmer, W.T., Gandin, V., Hanna, E., Zong, R., Barbon, A., Nelson, D.L., et al. (2014). FXR1P limits long-term memory, long-lasting synaptic potentiation, and de novo GluA2 translation. *Cell Rep.* **9**, 1402–1416.

Davies, M.H., Stempel, A.J., and Powers, M.R. (2008). MCP-1 deficiency delays regression of pathologic retinal neovascularization in a model of ischemic retinopathy. *Invest. Ophthalmol. Vis. Sci.* **49**, 4195–4202.

Drake, A.J., and Reynolds, R.M. (2010). Impact of maternal obesity on offspring obesity and cardiometabolic disease risk. *Reproduction* **140**, 387–398.

El Kaoutari, A.E., Armougom, F., Gordon, J.I., Raoult, D., and Henrissat, B. (2013). The abundance and variety of carbohydrate-active enzymes in the human gut microbiota. *Nat. Rev. Microbiol.* **11**, 497–504.

Erny, D., Hrabě de Angelis, A.L., Jaitin, D., Wieghofer, P., Staszewski, O., David, E., Keren-Shaul, H., Mhlahoi, T., Jakobshagen, K., Buch, T., et al. (2015). Host microbiota constantly control maturation and function of microglia in the CNS. *Nat. Neurosci.* **18**, 965–977.

Ferretti, P., Pasolli, E., Tett, A., Asnicar, F., Gorfer, V., Fedi, S., Armanini, F., Truong, D.T., Manara, S., Zolfo, M., et al. (2018). Mother-to-infant microbial transmission from different body sites shapes the developing infant gut microbiome. *Cell Host Microbe* **24**, 133–145.e5.

Frazee, A.C., Perte, G., Jaffe, A.E., Langmead, B., Salzberg, S.L., and Leek, J.T. (2014). Flexible isoform-level differential expression analysis. *Nat. Biotechnol.* **33**, 243–246.

Frazee, A.C., Perte, G., Jaffe, A.E., Langmead, B., Salzberg, S.L., and Leek, J.T. (2015). Ballgown bridges the gap between transcriptome assembly and expression analysis. *Nat. Biotechnol.* **33**, 243–246.

Frick, L.R., Williams, K., and Pittenger, C. (2013). Microglial dysregulation in psychiatric disease. *Clin. Dev. Immunol.* **2013**, 608654.

Frost, G., Sleeth, M.L., Sahuri-Arisoylu, M., Lizarbe, B., Cerdan, S., Brody, L., Anastasovska, J., Ghourab, S., Hankir, M., Zhang, S., et al. (2014). The short-chain fatty acid acetate reduces appetite via a central homeostatic mechanism. *Nat. Commun.* **5**, 3611.

Gandal, M.J., Zhang, P., Hadjichristou, E., Walker, R.L., Chen, C., Liu, S., Won, H., van Bakel, H., Varghese, M., Wang, Y., et al. (2018). Transcriptome-wide isoform-level dysregulation in ASD, schizophrenia, and bipolar disorder. *Science* **362**, eaat8127.

Gibson, G.R. (1999). Dietary modulation of the human gut microflora using the prebiotics oligofructose and inulin. *J. Nutr.* **129**, 1438S–1441S.

Godfrey, K.M., Reynolds, R.M., Prescott, S.L., Nyirenda, M., Jaddoe, V.W., Eriksson, J.G., and Broekman, B.F. (2017). Influence of maternal obesity on the long-term health of offspring. *Lancet Diabetes Endocrinol.* **5**, 53–64.

Gonatosopoulos-Pournatzis, T., Wu, M., Braunschweig, U., Roth, J., Han, H., Best, A.J., Raj, B., Aregger, M., O'Hanlon, D., Ellis, J.D., et al. (2018). Genome-wide CRISPR-Cas9 interrogation of splicing networks reveals a mechanism for recognition of autism-misregulated neuronal microexons. *Mol. Cell* **72**, 510–524.e12.

Guo, W., Polich, E.D., Su, J., Gao, Y., Christopher, D.M., Allan, A.M., Wang, M., Wang, F., Wang, G., and Zhao, X. (2015). Fragile X proteins FMRP and FXR2P control synaptic GluA1 expression and neuronal maturation via distinct mechanisms. *Cell Rep.* **11**, 1651–1666.

Hanson, M., Barker, M., Dodd, J.M., Kumanyika, S., Norris, S., Steegers, E., Stephenson, J., Thangaratinam, S., and Yang, H. (2017). Interventions to prevent maternal obesity before conception, during pregnancy, and post partum. *Lancet Diabetes Endocrinol.* **5**, 65–76.

Harris, J.E., Pinckard, K.M., Wright, K.R., Baer, L.A., Arts, P.J., Abay, E., Shettigar, V.K., Lehnig, A.C., Robertson, B., Madaris, K., et al. (2020). Exercise-induced 3'-sialyllactose in breast milk is a critical mediator to improve metabolic health and cardiac function in mouse offspring. *Nat. Metab.* **2**, 678–687.

Heslehurst, N., Rankin, J., Wilkinson, J.R., and Summerbell, C.D. (2010). A nationally representative study of maternal obesity in England, UK: trends in incidence and demographic inequalities in 619 323 births, 1989–2007. *Int. J. Obes.* **34**, 420–428.

Hsiao, E.Y., McBride, S.W., Hsien, S., Sharon, G., Hyde, E.R., McCue, T., Codelli, J.A., Chow, J., Reisman, S.E., Petrosino, J.F., et al. (2013). Microbiota modulate behavioral and physiological abnormalities associated with neurodevelopmental disorders. *Cell* **155**, 1451–1463.

- Kaifu, T., Nakahara, J., Inui, M., Mishima, K., Momiyama, T., Kaji, M., Sugahara, A., Koito, H., Ujike-Asai, A., Nakamura, A., et al. (2003). Osteopetrosis and thalamic hypomyelination with synaptic degeneration in DAP12-deficient mice. *J. Clin. Invest.* *111*, 323–332.
- Kang, S.S., Kurti, A., Fair, D.A., and Fryer, J.D. (2014). Dietary intervention rescues maternal obesity induced behavior deficits and neuroinflammation in offspring. *J. Neuroinflamm.* *11*, 156.
- Kim, D., Langmead, B., and Salzberg, S.L. (2015). HISAT: a fast spliced aligner with low memory requirements. *Nat. Methods* *12*, 357–360.
- Kimura, I., Miyamoto, J., Ohue-Kitano, R., Watanabe, K., Yamada, T., Onuki, M., Aoki, R., Isobe, Y., Kashihara, D., Inoue, D., et al. (2020). Maternal gut microbiota in pregnancy influences offspring metabolic phenotype in mice. *Science* *367*, eaaw8429.
- Kratsman, N., Getselter, D., and Elliott, E. (2016). Sodium butyrate attenuates social behavior deficits and modifies the transcription of inhibitory/excitatory genes in the frontal cortex of an autism model. *Neuropharmacology* *102*, 136–145.
- Lagkouvardos, I., Lesker, T.R., Hitch, T.C.A., Gálvez, E.J.C., Smit, N., Neuhaus, K., Wang, J., Baines, J.F., Abt, B., Stecher, B., et al. (2019). Sequence and cultivation study of Muribaculaceae reveals novel species, host preference, and functional potential of this yet undescribed family. *Microbiome* *7*, 28.
- Li, F., Yang, X.J., Cao, Y.C., Li, S.X., Yao, J.H., Li, Z.J., and Sun, F.F. (2014). Effects of dietary effective fiber to rumen degradable starch ratios on the risk of sub-acute ruminal acidosis and rumen content fatty acids composition in dairy goat. *Anim. Feed Sci. Technol.* *189*, 54–62.
- Li, B., He, Y., Ma, J., Huang, P., Du, J., Cao, L., Wang, Y., Xiao, Q., Tang, H., and Chen, S. (2019). Mild cognitive impairment has similar alterations as Alzheimer's disease in gut microbiota. *Alzheimers Dement.* *15*, 1357–1366.
- Liu, Q., Chen, Y., Shen, C., Xiao, Y., Wang, Y., Liu, Z., and Liu, X. (2017). Chicoric acid supplementation prevents systemic inflammation-induced memory impairment and amyloidogenesis via inhibition of NF- κ B. *FASEB J.* *31*, 1494–1507.
- Liu, F., Li, J., Wu, F., Zheng, H., Peng, Q., and Zhou, H. (2019). Altered composition and function of intestinal microbiota in autism spectrum disorders: a systematic review. *Transl. Psychiatr.* *9*, 43.
- Liu, Z., Dai, X., Zhang, H., Shi, R., Hui, Y., Jin, X., Zhang, W., Wang, L., Wang, Q., Wang, D., et al. (2020). Gut microbiota mediates intermittent-fasting alleviation of diabetes-induced cognitive impairment. *Nat. Commun.* *11*, 855.
- Lohman, T.G., Roche, A.F., and Martorell, R. (1988). *Anthropometric Standardization Reference Manual* (Human Kinetics Publishers Books).
- Lueptow, L.M. (2017). Novel object recognition test for the investigation of learning and memory in mice. *J. Vis. Exp.* *126*, e55718.
- Ma, J., Prince, A.L., Bader, D., Hu, M., Ganu, R., Baquero, K., Blundell, P., Harris, AlanR., Frias, A.E., Grove, K.L., et al. (2014). High-fat maternal diet during pregnancy persistently alters the offspring microbiome in a primate model. *Nat. Commun.* *5*, 3889.
- Magoc, T., and Salzberg, S.L. (2011). FLASH: fast length adjustment of short reads to improve genome assemblies. *Bioinformatics* *27*, 2957–2963.
- Martin, V., Allaili, N., Euvrard, M., Marday, T., Riffaud, A., Franc, B., Mocaër, E., Gabriel, C., Fossati, P., Lehericy, S., and Lanfumey, L. (2017). Effect of agomelatine on memory deficits and hippocampal gene expression induced by chronic social defeat stress in mice. *Sci. Rep.* *8*, 45907.
- Messaoudi, M., Rozan, P., Nejdí, A., Hidalgo, S., and Desor, D. (2005). Behavioural and cognitive effects of oligofructose-enriched inulin in rats. *Br. J. Nutr.* *93*, S27–S30.
- Moeller, A.H., Suzuki, T.A., Phifer-Rixey, M., and Nachman, M.W. (2018). Transmission modes of the mammalian gut microbiota. *Science* *362*, 453–457.
- Ormerod, K.L., Wood, D.L., Lachner, N., Gellatly, S.L., Daly, J.N., Parsons, J.D., Dal'Molin, C.G., Palfreyman, R.W., Nielsen, L.K., Cooper, M.A., et al. (2016). Genomic characterization of the uncultured Bacteroidales family S24-7 inhabiting the guts of homeothermic animals. *Microbiome* *4*, 36.
- Park, J.Y., Choi, J., Lee, Y., Lee, J.E., Lee, E.H., Kwon, H.J., Yang, J., Jeong, B.R., Kim, Y.K., and Han, P.L. (2017). Metagenome analysis of bodily micro-
- biota in a mouse model of Alzheimer disease using bacteria-derived membrane vesicles in blood. *Exp. Neurobiol.* *26*, 369–379.
- Pertea, M., Pertea, G.M., Antonescu, C.M., Chang, T.C., Mendell, J.T., and Salzberg, S.L. (2015). StringTie enables improved reconstruction of a transcriptome from RNA-seq reads. *Nat. Biotechnol.* *33*, 290–295.
- Pluznick, J.L., Protzko, R.J., Gevorgyan, H., Peterlin, Z., Sipos, A., Han, J., Brunet, I., Wan, L.X., Rey, F., Wang, T., et al. (2013). Olfactory receptor responding to gut microbiota-derived signals plays a role in renin secretion and blood pressure regulation. *Proc. Natl. Acad. Sci. USA* *110*, 4410–4415.
- Poston, L., Caleyachetty, R., Cnattingius, S., Corvalán, C., Uauy, R., Herring, S., and Gillman, M.W. (2016). Preconceptional and maternal obesity: epidemiology and health consequences. *Lancet Diabetes Endocrinol.* *4*, 1025–1036.
- Pugh, S.J., Richardson, G.A., Hutcheon, J.A., Himes, K.P., Brooks, M.M., Day, N.L., and Bodnar, L.M. (2015). Maternal obesity and excessive gestational weight gain are associated with components of child cognition. *J. Nutr.* *145*, 2562–2569.
- Raverdeau, M., Gely-Pernot, A., Féret, B., Dennefeld, C., Benoit, G., Davidson, I., Chambon, P., Mark, M., and Ghyselinck, N.B. (2012). Retinoic acid induces Sertoli cell paracrine signals for spermatogonia differentiation but cell autonomously drives spermatocyte meiosis. *Proc. Natl. Acad. Sci. USA* *109*, 16582–16587.
- Rydbirk, R., Folke, J., Winge, K., Aznar, S., Pakkenberg, B., and Brudek, T. (2016). Assessment of brain reference genes for RT-qPCR studies in neurodegenerative diseases. *Sci. Rep.* *6*, 37116.
- Salter, M.W., and Stevens, B. (2017). Microglia emerge as central players in brain disease. *Nat. Med.* *23*, 1018–1027.
- Sandoval-Motta, S., Aldana, M., Martínez-Romero, E., and Frank, A. (2017). The human microbiome and the missing heritability problem. *Front. Genet.* *8*, 80.
- Sarker, G., and Peleg-Raibstein, D. (2018). Maternal overnutrition induces long-term cognitive deficits across several generations. *Nutrients* *11*, 7.
- Shala, M., and Dharmo, M. (2013). Prevalence of behavioural and emotional problems among two to five years old Kosovar preschool children—parent's report. *Psychology* *04*, 1008–1013.
- Shimizu, Y., Amano, H., Ito, Y., Betto, T., Yamane, S., Inoue, T., Nishizawa, N., Matsui, Y., Kamata, M., Nakamura, M., et al. (2017). Angiotensin II subtype 1a receptor signaling in resident hepatic macrophages induces liver metastasis formation. *Cancer Sci.* *108*, 1757–1768.
- Sonnenburg, E.D., and Sonnenburg, J.L. (2014). Starving our microbial self: the deleterious consequences of a diet deficient in microbiota-accessible carbohydrates. *Cell Metab.* *20*, 779–786.
- State, M.W. (2010). Another piece of the autism puzzle. *Nat. Genet.* *42*, 478–479.
- Sunkaria, A., Yadav, A., Bhardwaj, S., and Sandhir, R. (2017). Postnatal protease inhibition promotes amyloid- β aggregation in hippocampus and impairs spatial learning in adult mice. *Neuroscience* *367*, 47–59.
- Thorburn, A.N., Macia, L., and Mackay, C.R. (2014). Diet, metabolites, and "western-lifestyle" inflammatory diseases. *Immunity* *40*, 833–842.
- Walter, T.J., and Crews, F.T. (2017). Microglial depletion alters the brain neuro-immune response to acute binge ethanol withdrawal. *J. Neuroinflamm.* *14*, 86.
- Wang, J., Zou, Q., Suo, Y., Tan, X., Yuan, T., Liu, Z., and Liu, X. (2019). Lycopene ameliorates systemic inflammation-induced synaptic dysfunction via improving insulin resistance and mitochondrial dysfunction in the liver-brain axis. *Food Funct.* *10*, 2125–2137.
- Wang, S., Harvey, L., Martin, R., van der Beek, E.M., Knol, J., Cryan, J.F., and Renes, I.B. (2018). Targeting the gut microbiota to influence brain development and function in early life. *Neurosci. Biobehav. R.* *95*, 191–201.
- Wang, Y., Li, N., Yang, J.J., Zhao, D.-M., Chen, B., Zhang, G.-Q., Chen, S., Cao, R.-F., Yu, H., Zhao, C.-Y., et al. (2020). Probiotics and fructo-oligosaccharide intervention modulate the microbiota-gut brain axis to improve autism spectrum reducing also the hyper-serotonergic state and the dopamine metabolism disorder. *Pharmacol. Res.* *157*, 104784.
- Wong, S.H., Zhao, L., Zhang, X., Nakatsu, G., Han, J., Xu, W., Xiao, X., Kwong, T.N.Y., Tsoi, H., Wu, W.K.K., et al. (2017). Gavage of fecal samples from patients with colorectal cancer promotes intestinal carcinogenesis in germ-free and conventional mice. *Gastroenterology* *153*, 1621–1633.e6.

Xiao, X., Nakatsu, G., Jin, Y., Wong, S., Yu, J., and Lau, J.Y. (2017). Gut microbiota mediates protection against enteropathy induced by indomethacin. *Sci. Rep.* 7, 40317.

Yassour, M., Jason, E., Hogstrom, L.J., Arthur, T.D., Tripathi, S., Siljander, H., Selvenius, J., Oikarinen, S., Hyöty, H., Virtanen, S.M., et al. (2018). Strain-level analysis of mother-to-child bacterial transmis-

sion during the first few months of life. *Cell Host Microbe* 24, 146–154.e4.

Zhang, X., Zou, Q., Zhao, B., Zhang, J., Zhao, W., Li, Y., Liu, R., Liu, X., and Liu, Z. (2020). Effects of alternate-day fasting, time-restricted fasting and intermittent energy restriction DSS-induced on colitis and behavioral disorders. *Redox Biol.* 32, 101535.

STAR★METHODS

KEY RESOURCES TABLE

REAGENT or RESOURCE	SOURCE	IDENTIFIER
Antibodies		
Rabbit monoclonal anti-PSD-95 (1:200)	Abcam	Cat# ab18258; RRID: AB_444362
Rabbit monoclonal anti-BDNF (1:200)	Abcam	Cat# ab226843; RRID: AB_2889875
Goat anti-Rabbit IgG (H+L) Cross-Adsorbed Secondary Antibody, HRP	Proteintech	Cat# SA00013-4; RRID: AB_2810984
Chemicals, Peptides, and Recombinant Proteins		
Inulin	Shanghai yuanye Bio-Technology	Cat# S11143
Metronidazole	Dalian Meilun Biological Technology Co.	Cat# MB2200
Ampicillin sulfate	DIYbio	Cat# DY80103
Vancomycin hydrochloride	DIYbio	Cat# DY80111
Neomycin sulfate	MP biomedicals	Cat# 100541
Mounting Medium (with DAPI)	Solarbio	Cat# S2110
Crotonic acid	Sigma-Aldrich	Cat# 113018
Acetic acid	Aladdin	Cat# A116173
Propionic acid	Aladdin	Cat# P110446
Butyric acid	Aladdin	Cat# B110438
Sodium acetate	Solarbio	Cat# S49014
Sodium propionate	Solarbio	Cat# S30148
TriZol	Invitrogen	Cat# T9424
LR-White resin	London Resin Company	Cat# 14381-UC
Critical Commercial Assays		
TIANamp Stool DNA Kit	TIANGEN	Cat# DP328-02
E.Z.N.A. Stool DNA Kit for 16S rRNA-seq	Omega	Cat# D4015
Evo M-MLV RT Kit	Accurate Biotechnology (Hunan)	Cat# AG11705
TB Green Premix Ex Taq II	TaKaRa	Cat# RR820Q
RNAiso Plus	TaKaRa	Cat# 9109
Qubit dsDNA BR Assay kit	Invitrogen	Cat# Q32853
Deposited Data		
Raw and processed data (RNA-seq)	GEO (http://www.ncbi.nlm.nih.gov/geo/)	GEO: GSE154434
Raw and processed data (16S rRNA-seq)	NCBI BioProject (https://www.ncbi.nlm.nih.gov/bioproject/)	PRJNA643672
Other raw data	Mendeley Data	https://doi.org/10.17632/f7xnz3ns84.1
Experimental Models: Organisms/Strains		
Mice: C57BL/6J	Xi'an Jiaotong University	N/A
Oligonucleotides		
Primers for qPCR, See Table S3	This paper	N/A
Software and Algorithms		
ImageJ (v1.42)	National Institutes of Health	RRID: SCR_003070
Supermaze	XR-Xmaze	http://www.softmaze.com/
R (v3.2.1)	R Team	https://www.r-project.org/
R (v3.5.2)	R Team	https://www.r-project.org/
GraphPad Prism 7.0	GraphPad Software	https://www.graphpad.com/scientificsoftware/prism/
Fast Length Adjustment of Short reads (v1.2.11)	(Magoč and Salzberg, 2011)	https://www.mybiosoftware.com/flash-1-0-2-fast-length-adjustment-short-reads.html

(Continued on next page)

Continued

REAGENT or RESOURCE	SOURCE	IDENTIFIER
USEARCH (v7.0.1090)	N/A	http://www.drive5.com/usearch/
UCHIME (v4.2.40)	N/A	http://www.drive5.com/uchime/uchime_download.html
Ribosomal Database Project Classifier (v2.2)	N/A	http://rdp.cme.msu.edu/
Trimmomatic (v 0.38)	N/A	https://omictools.com/trimmomatic-tool
Hisat2 (v 2- 2.1.0)	(Kim et al., 2015)	http://daehwankimlab.github.io/hisat2/
StringTie (v 1.3.4d.)	(Pertea et al., 2015)	https://ccb.jhu.edu/software/stringtie/history.shtml
Ballgown (v 2.12.0)	(Frazee et al., 2014, 2015)	http://bioconductor.riken.jp/packages/3.7/bioc/html/ballgown.html
GSEA (v 4.0.3)	N/A	https://www.gsea-msigdb.org/gsea/index.jsp
Greengenes database (v 201305)	N/A	http://greengenes.secondgenome.com/
KEGG pathway database	N/A	https://www.kegg.jp/keggbin/search_pathway_text?map=mmu&keyword=&mode=1&viewImage=truehttps://www.kegg.jp/kegg
OriginPro 2018C	OriginLab Corporation	https://www.originlab.com
IBM SPSS program (v 22)	International Business Machines Corporation	https://www.ibm.com/products/spss-statistics
Other		
Control diet	Trophic Animal Feed High-Tech	LAD 3001G
Inulin-enriched control diet	Trophic Animal Feed High-Tech	TP 23300-X1
High-fat diet	Trophic Animal Feed High-Tech	TP 23300
Inulin-enriched high fat diet	Trophic Animal Feed High-Tech	TP 23300-X2

RESOURCE AVAILABILITY**Lead contact**

Further information and requests for resources and reagents should be directed to and will be fulfilled by the Lead Contact, Xuebo Liu (xueboliu@nwsuaf.edu.cn).

Materials availability

This study did not generate new unique reagents.

Data and code availability

The raw data of RNA sequencing in the current study were deposited on GEO <http://www.ncbi.nlm.nih.gov/geo/>, and the accession number is GEO: GSE154434. The accession number for the entire 16S rRNA sequencing dataset reported in this manuscript is NCBI BioProject: [PRJNA643672](https://www.ncbi.nlm.nih.gov/bioproject/) <https://www.ncbi.nlm.nih.gov/bioproject/>.

Original data have been deposited to Mendeley Data: <https://doi.org/10.17632/f7xnz3ns84.1>

EXPERIMENTAL MODEL AND SUBJECT DETAILS**Human study**

Participants were 778 children (403 boys and 375 girls) aged 7-14 years (mean age=10.4 ± 1.9) recruited from four primary schools in Taizhou and Wuxi, China. Sampling took place in classes that were randomly selected from each grade in the selected schools, where children and their parents were enrolled to complete a series of questionnaires. Those with a serious organic disease, abnormal physical development, or physical impairments were excluded from this study. The questionnaire included information on the child's age, sex, body weight, height, physical activity, sleep time, birth weight, breastfeeding history, maternal weight before pregnancy, weight gain during pregnancy, height, parental education level, family income, and a questionnaire of the Child Behavior Checklist (CBCL) (Shala and Dharmo, 2013). Anthropometric measures followed standardized protocols (Lohman et al., 1988). Parents completed the social competence scale of the CBCL, which includes 20 social competence items that comprise three social competence subscales that measure the following competencies: activities (e.g., sports, hobbies); social subjects (e.g., friendships, interpersonal skills); and school performance (e.g., performance, ability, school problems) (Shala and Dharmo, 2013). The total social

competence score was the sum of these three subscales. This study was approved by the Ethics Committee of School of Public Health of Shanghai Jiao Tong University for Human Subject Research, and all parents gave written informed consent, No. SJUPN-201815.

Animal study

Both C57BL/6J male and female mice were obtained from Xi'an Jiaotong University (Xi'an, Shaanxi, China) at 7 weeks of age. Then mice were housed in the Northwest A&F University animal facility under standard conditions, with a strict 12 h light/dark cycle (8:00 a.m. to 8:00 p.m.), humidity at $50 \pm 15\%$, a temperature of $22 \pm 2^\circ\text{C}$, and *ad libitum* access to food and water. Before the experiment, all mice were maintained on chow, which we considered as a control diet. The maternal mice were randomly assigned to different experimental groups. During the experiment, animal caretakers and investigators conducting the experiments were blinded to the group allocation of mice. The health status of mice was determined via daily observation by technicians supported by veterinary care. All of the experimental procedures were followed using the Guide for the Care and Use of Laboratory Animals: Eighth Edition (ISBN-10: 0-309-15396-4). We have complied with all relevant ethical regulations for animal testing, and research and protocols and protocols were approved by the Northwest A&F University and BGI Institutional Review Board on Bioethics and Biosafety (BGI-IRB).

Dietary fiber treatment

For maternal dietary fiber treatment, female mice were randomly allocated to one of the four following diets: control diet (mCD; LAD 3001G; Trophic Animal Feed High-tech, Nantong, China), high-fat diet (mHFD; TP 23300; Trophic Animal Feed High-tech, Nantong, China), a HFD with 37 g inulin per 1000 kcal as a source of fiber (mFFD; TP 23300-X2; Trophic Animal Feed High-tech, Nantong, China), and a control diet with inulin as a source of fiber (mFD; TP 23300-X1; Trophic Animal Feed High-tech, Nantong, China) for 10-12 weeks. The HFD and FFD are isocaloric. The mCD and mFD diets consisted of 16.7% kcal from fat, 63.9% kcal from carbohydrates, and 19.4% kcal from protein. The mHFD and mFFD diets consisted of 60% kcal from fat, 20.6% kcal from carbohydrates, and 19.4% kcal from protein. The composition of all purified-ingredient diets used in this study is listed in Table S2. Female mice were housed five to a cage and weight was measured every six days before pregnancy. After 12 weeks on the respective diets, female mice were paired with C57BL/6J adult male mice fed chow to produce subject offspring (2 females:1 male). Pregnant dams were single-housed, and their offspring were weaned at 3 weeks of age. At weaning, different litters born within up to a week apart were combined and housed in a cage of 4-5 male or female mice per cage, and all were placed on a control diet (-oCD), regardless of the maternal diet (mCD, mHFD, mFFD, or mFD). $n=7-9$ offspring from 5-7 litters per group, 1-3 offspring per litter (the numbers of offspring and litters are specified in the figure legends).

For dietary fiber treatment to offspring, both female and male offspring from the mHFD and mCD dams were switched to an inulin-containing diet (-oFD) at 3 weeks old until they were aged 8 to 10 weeks. $n=8-9$ offspring from 4-5 litters per group, 1-3 offspring per litter (the numbers of offspring and litters are specified in the figure legends).

All behavioral tests were performed in 8- to 10-week-old male and female mice. Offspring of at least three litters (\geq three different mothers) in each group were analyzed in individual experiments. During the subsequent analyses, investigators assessing, measuring, or quantifying experimental outcomes were blinded to the intervention group.

METHOD DETAILS

Microbiota depletion

In brief, mice were treated with an antibiotic solution (ATB) containing 0.5 g/L vancomycin hydrochloride, 1 g/L neomycin sulfate, 1 g/L ampicillin sulfate, and 1 g/L metronidazole added into their sterile drinking water. Solutions and bottles were changed once weekly. Mice received 14 days of ATB before undergoing fecal microbial transplantation. Microbiota depletion was confirmed by plating feces on BHI agar plates under anaerobic and aerobic conditions, and quantitative real-time PCR (qRT-PCR). qRT-PCR was performed with the universal bacteria-specific primer:

(8F: AGAGTTTGATCCTGGCTCAG; 338R: CTGCTGCCTCCCGTAGGAGT).

Gut microbiota transplantation

Microbiota transplantation was done according to a previous study (Wong et al., 2017). To prepare the sample for gavage, the fecal samples from donor mice from the four diet groups (dCD, dFD, dHFD, and dFFD, 4-8 mice per group) were collected and mixed at equal weight with fecal samples of mice within the same diet group. Briefly, fresh fecal samples were resuspended in sterile PBS (15 mL/g of feces) and were then vigorously vortexed for 5 min, followed by 5-min standing to precipitate particles. Supernatants were then used to colonize ATB mice by 3 consecutive days of oral gavage (200 μL /mouse). Colonized mice (rCD, rFD, rHFD, and rFFD) were subsequently mated with C57BL/6J male 3 days after colonization. All pregnant mice were gavaged twice weekly during pregnancy and lactation. The colonization was confirmed by plating feces on BHI agar plates on anaerobic and aerobic conditions. $n=14-17$ offspring from 4-7 litters per group, 1-6 offspring per litter (the numbers of offspring and litters are specified in the figure legends).

Cross-fostering

The fecal microbiota from female donor (dHFD and dFFD) mice were transplanted into antibiotic-treated adult female mice (rHFD and rFFD). Pregnant mice (rHFD and rFFD) were monitored every day, and immediately after birth (the day on which pups were born was considered P0). Pups were cross-fostered between P0 and P1 all the pups of rHFD dams were housed with lactating rFFD dams. Similarly, same-day born pups of rFFD dams were housed with lactating rHFD dams. After 3 weeks, the cross-fostered pups were weaned and all placed on a control diet (-oCD). All behavioral tests were performed in 8- to 10-week-old male and female mice. $n=13-14$ offspring from 3 litters per group, 3-7 offspring per litter (the numbers of offspring and litters are specified in the figure legends).

Co-housing

For the co-housing experiments, sex-matched offspring from mHFD and mFFD dams were co-housed (3 weeks old) in gang cages at a ratio of 2:3 until they were 8 to 10 weeks old, which is when behavioral tests were performed. $n=6-12$ offspring from 3-6 litters per group, 1-4 offspring per litter (the numbers of offspring and litters are specified in the figure legends).

SCFAs treatment

Both female and male offspring (3 weeks old) from mHFD dams were treated with a mixture of sodium acetate (67.5 mM) and sodium propionate (22.5 mM) in drinking water until the age of 8 to 10 weeks, at which time behavioral tests were performed. Mice consumed the treated water *ad libitum* over the treatment period. $n=7-14$ offspring from 4-6 litters per group, 1-4 offspring per litter (the numbers of offspring and litters are specified in the figure legends).

Y-maze

The Y-maze task was performed as previously described (Arai et al., 2001) to assess spontaneous alternation, which was defined as successive entries into the three arms in overlapping triplet sets. The maze was made up of three arms, each of which was 35 cm long, 15 cm high, and 5 cm wide, and converged to an equal angle (Shanghai Xinruan Information Technology, Shanghai, China). The mouse was placed in the center of the apparatus and was allowed to explore it for 8 min. The total numbers of arm entries and alternations were counted. The percent alternation was calculated as the ratio of actual to possible alternations (defined as the total number of arm entries -2) \times 100%.

Novel object recognition

The novel object recognition test is a relatively low-stress and efficient method to test long-term learning and memory in mice (Luep-tow, 2017). Given that mice have an innate preference for novelty, if a mouse recognizes the familiar object, it will spend most of its time at the novel object. The novel object recognition test was completed over 3 days, which included a habituation day, training day, and testing day.

On the habituation day, the mouse was removed from its home cage and placed in the middle of the empty open arena (40 \times 40 \times 40 cm) and allowed to freely explore the arena for 5 min. At the end of the session, the mouse was transferred to an empty holding cage, and put back in the home cage after all mice in the same home cage had been handled. On the training day, two identical objects were placed in the central symmetrical positions of the arena. The mouse was placed in the center of the arena, equidistant from the two identical objects. After freely exploring the two objects for 5 min, the mouse was transported to the holding cage. On the testing day, one of the training objects was replaced with a novel object, and the mouse was allowed to freely explore for 5 min. The discrimination index (d2) was calculated as the time spent exploring the novel object minus the time spent exploring the familiar object, divided by total exploration time.

Three-chamber social test

The three-chamber test for sociability and social novelty preference was performed as previously described (Buffington et al., 2016). Briefly, the mouse was first habituated to the full, empty arena for 5 min, which was a 60 \times 40 cm² plexiglass box divided into three equally sized, interconnected chambers (left, center, right).

In the second 5-min section, sociability was measured. During this period, the subject could interact either with an empty wire cup (empty) or an age- and sex-matched stranger conspecific contained in the other wire cup (mouse 1). The time spent interacting (sniffing, crawling upon) with either the empty cup or mouse 1 was recorded using tracking software (SuperMaze) by independent observers. Sociability index was calculated by the following: (time spent with mouse- time spent with empty cup)/ (time spent with mouse + time spent with empty cup).

Finally, preference for social novelty was assessed during a third 5-min period, by introducing a second stranger mouse (mouse 2) into the previously empty cup. The time spent interacting with either mouse 1 or mouse 2 was recorded using tracking software by independent observers. The index of social novelty preference was calculated by the following: (time spent with novel mouse- time spent with familiar mouse)/ (time spent with novel mouse+ time spent with familiar mouse).

16S rRNA microbiome sequencing

As the maternal and offspring dietary fiber treatment experiments were conducted simultaneously, the gut microbiome of mHFD-oCD and mCD-oCD group in Figures 2, 5, S4, and S6 are from same mouse fecal samples. Fecal samples were collected from

the respective groups before the behavioral tests and stored at -80°C until DNA extraction. The total cellular DNA was extracted with the E.Z.N.A. Stool DNA Kit (Omega, Norcross, GA, USA) according to the company instructions. Quantification of genomic DNA was verified using Qubit Fluorometer by using Qubit dsDNA BR Assay kit (Invitrogen, USA), and the quality was checked by running aliquot on 1% agarose gel. Qualified genomic DNA samples were processed for 16S rRNA library preparation. The bacterial hypervariable V3–V4 region of 16S rRNA was amplified by using primer: 341_F: 5'-ACTCCTACGGGAGGCAGCAG-3' and 806_R: 5'-GGACTACHVGGGTWTCTAAT-3'. The validated library was used for sequencing on HiSeq2500 (Illumina, CA, USA) and by generating 2×300 bp paired-end reads. The high quality paired-end reads were combined to tags based on overlaps by FLASH (Fast Length Adjustment of Short reads, v1.2.11), and then clustered into OTUs at a similarity cutoff value of 97% using USEARCH (v7.0.1090), and chimeric sequences were compared with Gold database using UCHIME (v4.2.40). OTU representative sequences were taxonomically classified using the Ribosomal Database Project Classifier (v2.2) with a minimum confidence threshold of 0.6, and were then mapped to the Greengenes database (v201305). The USEARCH_global was used to compare all Tags back to OTU to get the OTU abundance statistics table of each sample. Principal coordinates analysis was performed by R (v3.5.2) at the OTU level to calculate the unweighted and weighted UniFrac distance, followed by a PERMANOVA test (Vegan: Adonis) to detect differences between the intervention groups. Alpha diversity was analyzed using R (v3.2.1) at the OTU level using Wilcoxon rank-sum test. Differential abundance analysis was performed using the Wilcoxon rank-sum test. The correlation was determined by R (v3.5.2) with Spearman's rank correlations, followed by the cor.test for multiple comparison corrections. A p value <0.05 was considered significant.

Fecal SCFAs assay

The concentrations of SCFAs (acetate, propionate, and butyrate) were determined using gas chromatography. Approximately 150 mg of the fecal content sample was added to 1 mL water and vigorously vortexed. The samples were then mixed with 150 μL 50% H_2SO_4 and 1.6 mL diethyl ether. The suspensions were incubated on ice for 20 min to extract SCFAs, followed by centrifugation at 8000 rpm for 5 minutes at 4°C . Finally, the organic phase was collected and analyzed using a Shimadzu GC-2014C gas chromatograph (Shimadzu Corporation, Kyoto, Japan) equipped with a DB-FFAP capillary column (30 m \times 0.25 μm \times 0.25 mm) (Agilent Technologies, Wilmington, DE, USA) and flame ionization detector. The initial temperature was 50°C , which was maintained for 3 min and then raised to 130°C at $10^{\circ}\text{C}/\text{min}$, increased to 170°C at $5^{\circ}\text{C}/\text{min}$, increased to 220°C at $15^{\circ}\text{C}/\text{min}$, and held at this temperature for 3 min. The injector and the detector temperatures were 250°C and 270°C , respectively.

Serum SCFAs assay

The detection of fecal and serum levels of SCFAs was conducted as previously described (Li et al., 2014). To remove the solid particle and protein, serum sample (200 μL) was mixed with 25% metaphosphoric acid (100 μL). After standing for 4 h at 4°C , the mixture was centrifuged for 10 min at 13500 rpm at 4°C . 4 μL crotonic acid (12.5%, Sigma-Aldrich) was added to an aliquot (200 μL) of the supernatants. After vortexing and standing for 30 min, the mixture was filtered through a 0.45 μm nylon filter (EMD Millipore). The SCFAs was separated and quantified by gas chromatography (Agilent Technologies 7820 GC system) using a 30 m \times 0.25 mm \times 0.33 μm fused silica column (AE-FFAP; ATECH Technologies, China). The injector and detector temperatures were set at 200°C and 250°C , respectively. The column temperature was increased from 45°C to 150°C at $20^{\circ}\text{C}/\text{min}$ and held for 5 min.

RNA isolation and qRT-PCR

Total RNA was extracted from brain tissues using the RNAiso Plus (TaKaRa, Dalian, China). RNA concentrations were determined using NanoDrop 2000/2000C (Thermo Scientific; Waltham, MA, USA), and total RNA was reverse-transcribed into cDNA using the Evo M-MLV RT Kit with gDNA Clean (Hunan Accurate Biotechnology) for qRT-PCR according to the manufacturer's protocol using no more than 1 μg total RNA in 20 μL reactions. The mRNA expression was quantified using TB Green Premix Ex TaqII (TaKaRa) in a CFX96 Touch apparatus (Bio-Rad, Hercules, CA, USA) with the primers listed in the Table S3. The following conditions were used: 95°C for 10 min and 95°C for 15 s, followed by 40 cycles of 1 min at 60°C . Differences in transcript levels were quantified by normalizing each amplicon to GAPDH, and the relative gene expression was calculated using the $2^{-\Delta\Delta\text{Ct}}$ method.

RNA sequencing analysis

Brain tissue from the hippocampus was macro-dissected and stored at -80°C until DNA extraction. The total RNA was extracted using TriZol (Invitrogen, Carlsbad, VA, USA) according to the manufacturer's instructions, and was then qualified and quantified using a NanoDrop and Agilent 2100 bioanalyzer (Thermo Fisher Scientific, MA, USA). RNA sequencing libraries were prepared using BGISEQ-500 (BGI-Shenzhen, China). Then, the sequencing data were filtered and trimmed using Trimmomatic (v0.38) to obtain high quality clean-read data for sequence analysis. Clean reads were mapped to the *Mus musculus* genome sequence (<ftp://ftp.ncbi.nlm.nih.gov/> https://ftp.ncbi.nlm.nih.gov/genomes/all/GCF/000/001/635/GCF_000001635.27_GRCm39/) using Hisat2 (v2-2.1.0). The reads of each sample were then assembled into transcripts and compared with reference gene models using StringTie (v1.3.4d). We merged the 49 transcripts to obtain a consensus transcript using a StringTie-Merge program. Transcripts that did not exist in the CDS database of the *Mus musculus* genome were extracted to predict new genes. The gene expression FPKM values were calculated using StringTie, based on the consensus transcript. Differential expression analysis was performed using Ballgown (v2.12.0), an R programming-based tool designed to facilitate flexible differential expression analysis of RNA-Seq data. Only genes

with FPKM >1 were subjected to analysis, and the differential expression genes were determined (FDR- $p < 0.05$). After the gene expression FPKM values had been calculated using StringTie software, gene set enrichment analysis (GSEA) was performed on genes ranked by their differential expression using Signal2Noise using GSEA software (v4.0.3). The KEGG pathway database was downloaded from <https://www.genome.jp/kegg/pathway.html>. In this analysis, the normalized enrichment score and False Discovery Rate (FDR) were calculated for each gene set and compared between groups.

Immunofluorescence

Immunofluorescence staining was performed according to previously described methods (Liu et al., 2017). The fixed brain sections were exposed to the primary antibodies (anti-PSD-95 or anti-BDNF) at 4°C overnight. After washing three times in PBS, these slices were incubated with a biotinylated goat anti-rabbit IgG (H+L) cross-adsorbed secondary antibody at 37°C for 20 min. The sections were then washed six times, and then mounted with Mounting Medium (with DAPI). Immunofluorescence images were acquired using an inverted fluorescent microscope (Olympus, Tokyo, Japan) (×200). Proteins were visualized using the Image J software (National Institutes of Health, Scion Corporation, USA).

Transmission electron microscopy

A transmission electron microscope analysis was performed to assess the ultrastructure of synapses in the CA1 region of the hippocampus, as was performed in our previous research (Liu et al., 2020). In brief, the CA1 region was removed from the hippocampus and treated in a cold fixative solution comprising 2.5% glutaraldehyde (pH 7.2) at 4°C for 24 h. After washing with PBS (0.1 M, pH 7.2), the specimens were post-fixed in 1% OsO₄ (in 0.2M PBS, pH 7.2) at 4°C for 1.5 h. After washing again with PBS, the specimens were dehydrated for 15 min in a series of ethanol solutions (30%, 50%, 70%, 80%, 90% (v/v)), and then dehydrated in 100% (v/v) for 30 min twice. Samples were then infiltrated overnight in a mixture of LR-White resin (London Resin Company, Reading, UK) and alcohol (1:1, v/v), followed by infiltration with pure LR-White resin twice (for 6 h and 3 h, respectively) at room temperature. The samples were embedded in pure LR-White resin, and were then incubated at 60°C for 48 h. Ultrathin sections were obtained using a diamond knife on the Leica EM UC7 ultramicrotome (Leica, Nussloch, Germany), and then stained with 3% aqueous solution of UA for 10–15 min, and re-floated by 4% Pb solution for 8–10 min. Sections were observed under a JEM-1230 transmission electron microscope (JEOL, Tokyo, Japan) at 80 kV and were recorded using a side-inserted BioScan Camera Model 792 (Gatan, Pleasanton, California, USA). The measurement was performed using Image J analysis software (National Institutes of Health, Scion Corporation, USA) by experimenters who were blind to the treatment groups.

QUANTIFICATION AND STATISTICAL ANALYSIS

Statistical analysis is described in each figure legend. Data from both human and mouse study were assessed for normality of distribution using the Kolmogorov-Smirnov test. For human study, analyses were performed using the IBM SPSS program (v22). The significance level was set to 0.05 for all analyses. The Kruskal-Wallis test was used to examine differences in the scores of the total social competence, activities, social subjects and school performance between the maternal weight status groups before pregnancy. We have used the linear regression model with the adjustment for child's sex, child's weight status, maternal and parental educational levels, family incomes to control confounders in order to estimate β -coefficient with 95% CI for the associations of maternal pre-pregnancy overweightness and obesity with the total social competence, activities, social subjects and school performance of children. Associations of maternal pre-pregnancy body mass index status with participant characteristics were explored using χ^2 tests and Kruskal-Wallis tests.

For mouse study, 'n' refers to the individual animals and no mice were excluded. No power calculations were conducted to pre-determine appropriate mouse sample sizes. The number of animal replicates needed was chosen based on similar experiments. RNA sequencing was analyzed using Ballgown (v2.12.0) and GSEA software (v4.0.3). Analysis and data visualization of microbial populations were carried out in R with various packages, as described above. Other than for the RNA sequencing and gut microbiome data, statistical analyses were performed in GraphPad Prism 7.0 or OriginPro 2018C. An ANOVA with Tukey's multiple comparison test was used for parametric analysis of variance between groups; two-tailed paired Student's *t* tests were used for pairwise comparisons; two-tailed unpaired Student's *t* tests were used for comparing 2 groups. Data are presented as the mean \pm SEM and the median \pm interquartile range unless otherwise noted. $p < 0.05$ was considered to be statistically significant.

Supplemental information

**High-fiber diet mitigates maternal
obesity-induced cognitive and social
dysfunction in the offspring via gut-brain axis**

Xiaoning Liu, Xiang Li, Bing Xia, Xin Jin, Qianhui Zou, Zhenhua Zeng, Weiyang Zhao, Shikai Yan, Ling Li, Shufen Yuan, Shancen Zhao, Xiaoshuang Dai, Fei Yin, Enrique Cadenas, Rui Hai Liu, Beita Zhao, Min Hou, Zhigang Liu, and Xuebo Liu

SUPPLEMENTAL FIGURES

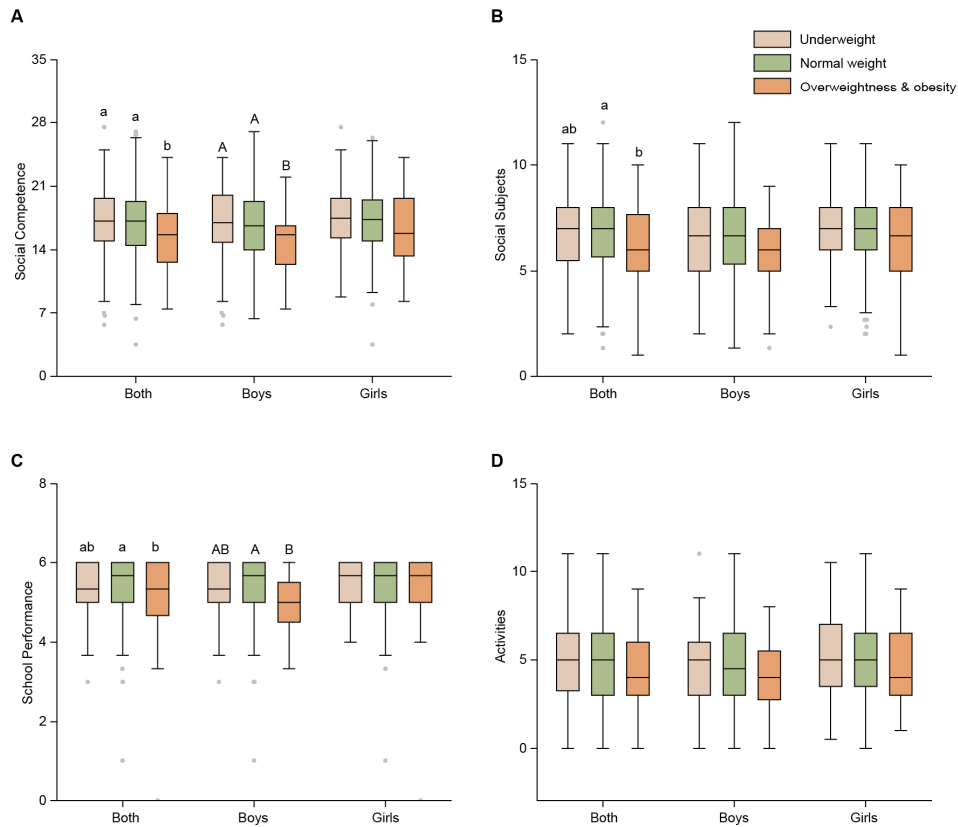


Figure S1 Maternal Prepregnancy Overweight and Obesity are Associated with Impaired Child Neurodevelopment, Related to Table 1

- (A) Social competence of the children.
- (B) Social subjects of the children.
- (C) School performance of the children.
- (D) Activities of the children.

Data are presented as the median ± interquartile range. For both (girls and boys), means with different letters (a, b) are significantly different from each

other ($p < 0.05$). For boys, means with different letters (A, B) are significantly different from each other ($p < 0.05$). Significant differences between mean values were determined using the Kruskal-Wallis test with Bonferroni's multiple comparisons.

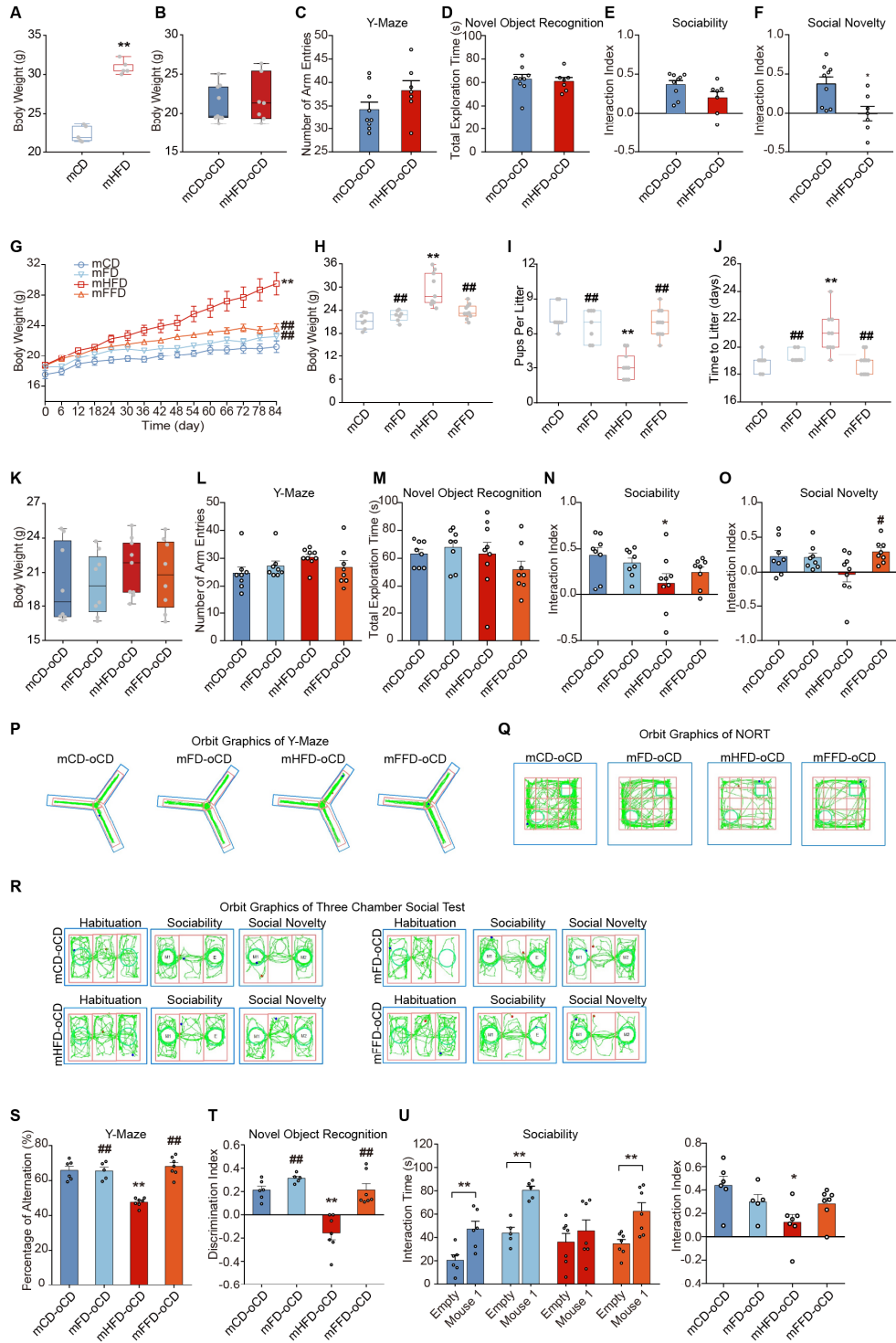


Figure S2 Maternal Obesity and Dietary Fiber Intake Impact the Weight of Mothers and Cognitive and Social Behaviors of Mouse Offspring, Related to Figure 1

(A) Body weight of dams after 12 weeks on a high-fat diet.

(B) Offspring weight at 8 weeks.

(C) The total number of arm entries in the Y-maze test.

(D) Total exploration time in the novel object recognition test.

(E-F) The index of sociability (E) and social novelty preference (F) in the three-chamber test.

(G-H) Body weight of dams over time (G) and after 12 weeks (H) on a high-fat diet.

(I-J) The litter size (I) and time to first litter (J).

(K) Offspring weight at 8 weeks of age.

(L) The total number of arm entries in the Y-maze test.

(M) Total exploration time in the novel object recognition test.

(N-O) The index of sociability (N) and social novelty preference (O) in the three-chamber test.

(P-R) The representative exploratory activity of mice in the Y-maze test (P), in the novel object recognition test (Q), and in the three-chamber test (R).

(S-U) When all offspring within the same litter were considered as $n=1$, behavioral phenotypes in offspring after maternal dietary fiber supplementation, including (S) Y-maze, (T) the novel object recognition test, and (U) sociability.

Data in (A-B) and (H-K) are presented as the median \pm interquartile range. Data in (C-G), (L-O), and (S-U) are presented as the mean \pm SEM. (B-F) mCD-oCD n=9 mice, 5 litters; mHFD-oCD n=7 mice, 5 litters. (K-O) mCD-oCD n=8 mice, 6 litters; mFD-oCD n=8 mice, 5 litters; mHFD-oCD n=9 mice, 7 litters; mFFD-oCD n=8 mice, 7 litters. Statistical analyses were performed by using two-tailed Student's t-tests (for A-F) or by using a one-way ANOVA with Tukey's multiple comparison test (for G-O and S-U). For dams, * p <0.05, ** p <0.01, compared with the mCD group, # p <0.05, ## p <0.01 versus the mHFD group. For offspring, * p <0.05, ** p <0.01, compared with the mCD-oCD group, # p <0.05, ## p <0.01 versus the mHFD-oCD group.

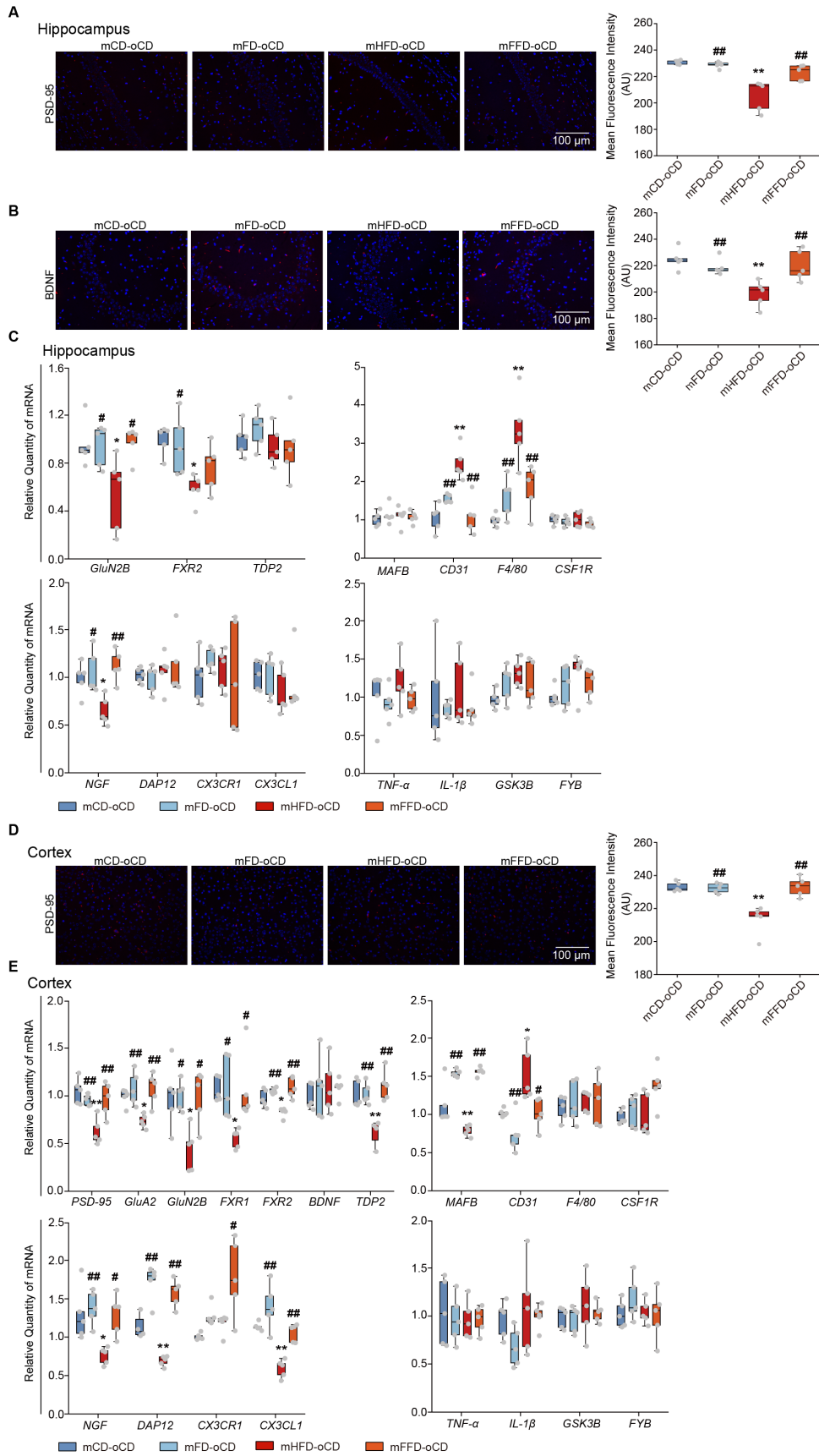


Figure S3 Dietary Fiber Intake Restored Maternal Obesity-induced Synaptic Damage and Disruption of Microglia Maturation in Offspring, Related to Figure 2

(A) Representative immunofluorescence images (left) and immunofluorescence intensity (right) of PSD-95 in the hippocampus.

(B) Representative immunofluorescence images (left) and immunofluorescence intensity (right) of BDNF in the hippocampus.

(C) The mRNA expressions of synapse-, microglia maturation-, and microglia function- related genes in the hippocampus.

(D) Representative immunofluorescence images (left) and immunofluorescence intensity (right) of PSD-95 in the prefrontal cortex.

(E) The mRNA expressions of synapse-, microglia maturation-, and microglia function- related genes in the prefrontal cortex.

Data are presented as the median \pm interquartile range. (A-E) n=5 mice, 5 litters/group. Statistical analyses were performed by using a one-way ANOVA with Tukey's multiple comparison test. * p <0.05, ** p <0.01, compared with the mCD-oCD group, # p <0.05, ## p <0.01 versus the mHFD-oCD group.

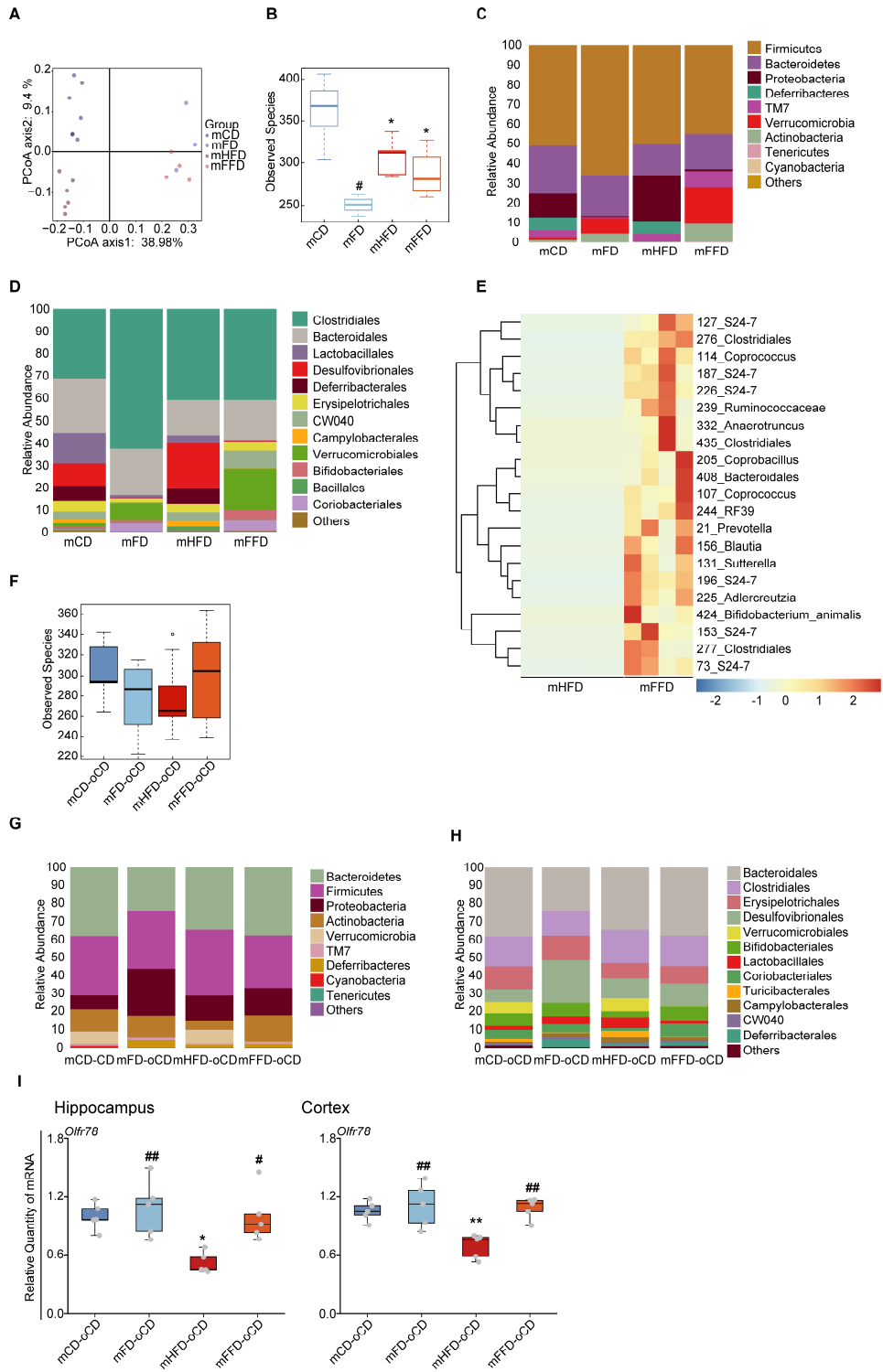


Figure S4 Dietary Fiber Intake Re-Shaped the Gut Microbiome in Both Mother and Offspring Mice, Related to Figure 2

(A) Principal coordinate analysis (PCoA) based on unweighted UniFrac distance and PERMANOVA (Adonis) was used to test the difference in gut microbiota composition and diversity between the groups of dams ($p < 0.001$, $R^2 = 0.52$; $n = 3-7$ mice/group).

(B) α -Diversity in dams was measured by observed operational taxonomic units (OTUs) from 16S rRNA gene sequencing. Differences between the treatment groups were tested using the Wilcoxon rank-sum test ($*p < 0.05$, $#p < 0.05$).

(C-D) The relative abundance of bacteria (C) at the phylum level and (D) at the order level in dams.

(E) A Z-score scaled heatmap of different OTUs identified by Wilcoxon rank-sum test between mHFD and mFFD with $p \leq 0.01$.

(F) α -Diversity in offspring was measured by observed OTUs. Differences between the treatment groups were tested using the Wilcoxon rank-sum test.

(G-H) The relative abundance of bacteria (G) at the phylum level and (H) at the order level in offspring.

(I) The mRNA expressions of *Olf78* in the hippocampus and prefrontal cortex ($n = 5$ mice, 5 litters/group).

Data are presented as the median \pm interquartile range. (F-I) mCD-oCD $n = 8$ mice, 6 litters; mFD-oCD $n = 8$ mice, 5 litters; mHFD-oCD $n = 9$ mice, 7 litters; mFFD-oCD $n = 8$ mice, 7 litters. The gut microbiome of mHFD-oCD and mCD-

oCD group in Figures 2, 5, S4, and S6 are from same mouse fecal samples. Statistical analyses were performed by using a one-way ANOVA with Tukey's multiple comparison test. For I, * $p < 0.05$, ** $p < 0.01$, compared with the mCD-oCD group, # $p < 0.05$, ## $p < 0.01$ versus the mHFD-oCD group.

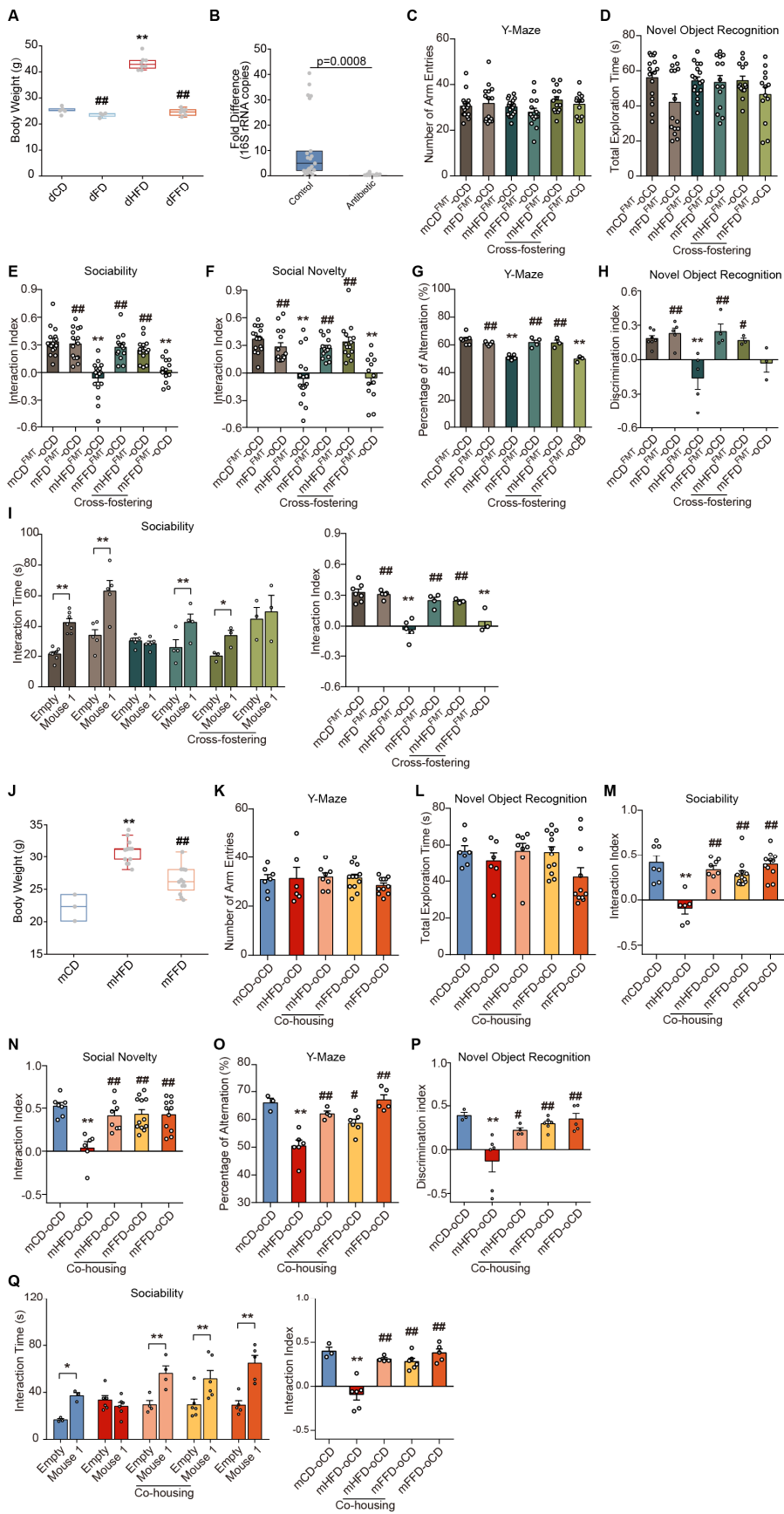


Figure S5 Gut Microbiota Mediated Maternal Obesity-induced Cognitive and Social Deficits in Offspring, Related to Figure 3

(A) Body weight of female mice donor fed one of four diets.

(B) qPCR of 16S rDNA analysis to ensure the removal efficacy of microbiota.

(C) The total number of arm entries of offspring from fecal microbiota-transplanted mothers in the Y-maze test.

(D) Total exploration time of offspring from fecal microbiota-transplanted mothers in the novel object recognition test.

(E-F) The index of sociability (E) and social novelty preference (F) in the three-chamber test.

(G-I) When all offspring within the same litter were considered as $n=1$, behavioral phenotypes in offspring from fecal microbiota-transplanted mothers, including (G) Y-maze, (H) the novel object recognition test, and (I) sociability.

(J) Body weight of dams, who gave birth to co-housed offspring.

(K) Total number of arm entries of co-housed offspring in the Y-maze test.

(L) Total exploration time of co-housed offspring in the novel object recognition test.

(M-N) The index of sociability (M) and social novelty preference (N) in the three-chamber test.

(O-Q) When all offspring within the same litter were considered as $n=1$, behavioral phenotypes in co-housed offspring, including (O) Y-maze, (P) the novel object recognition test, and (Q) sociability.

Data shown in (A-B) and (J) are presented as the median \pm interquartile range. Data shown in (C-I) and (K-Q) are presented as the mean \pm SEM. (C-F) mCD^{FMT}-oCD n=16 mice, 7 litters; mFD^{FMT}-oCD n=15, 5 litters; mHFD^{FMT}-oCD n=17 mice, 5 litters; mHFD^{FMT}-oCD (Cross-fostering) n=14 mice, 3 litters; mFFD^{FMT}-oCD (Cross-fostering) n =13 mice, 3 litters; mFFD-oCD n=14 mice, 4 litters. (K-N) mCD-oCD n=7 mice, 3 litters; mHFD-oCD n=6 mice 6 litters; mHFD-oCD (co-housing) n=8 mice, 4 litters; mFFD-oCD (co-housing) n= 12 mice, 6 litters; mFFD-oCD n= 11 mice, 5 litters. Statistical analyses were performed by using a one-way ANOVA with Tukey's multiple comparison test (for A and C-Q) or by using two-tailed Student's t-tests (for B). For A, * p <0.05, ** p <0.01, compared with the dCD group, # p <0.05, ## p <0.01 versus the dHFD group. For C-I, * p <0.05, ** p <0.01, compared with the mCD^{FMT}-oCD group, # p <0.05, ## p <0.01 versus the mHFD^{FMT}-oCD group. For J, * p <0.05, ** p <0.01, compared with the mCD group, # p <0.05, ## p <0.01 versus the mHFD group. For K-Q, * p <0.05, ** p <0.01, compared with the mCD-oCD group, # p <0.05, ## p <0.01 versus the mHFD-oCD group.

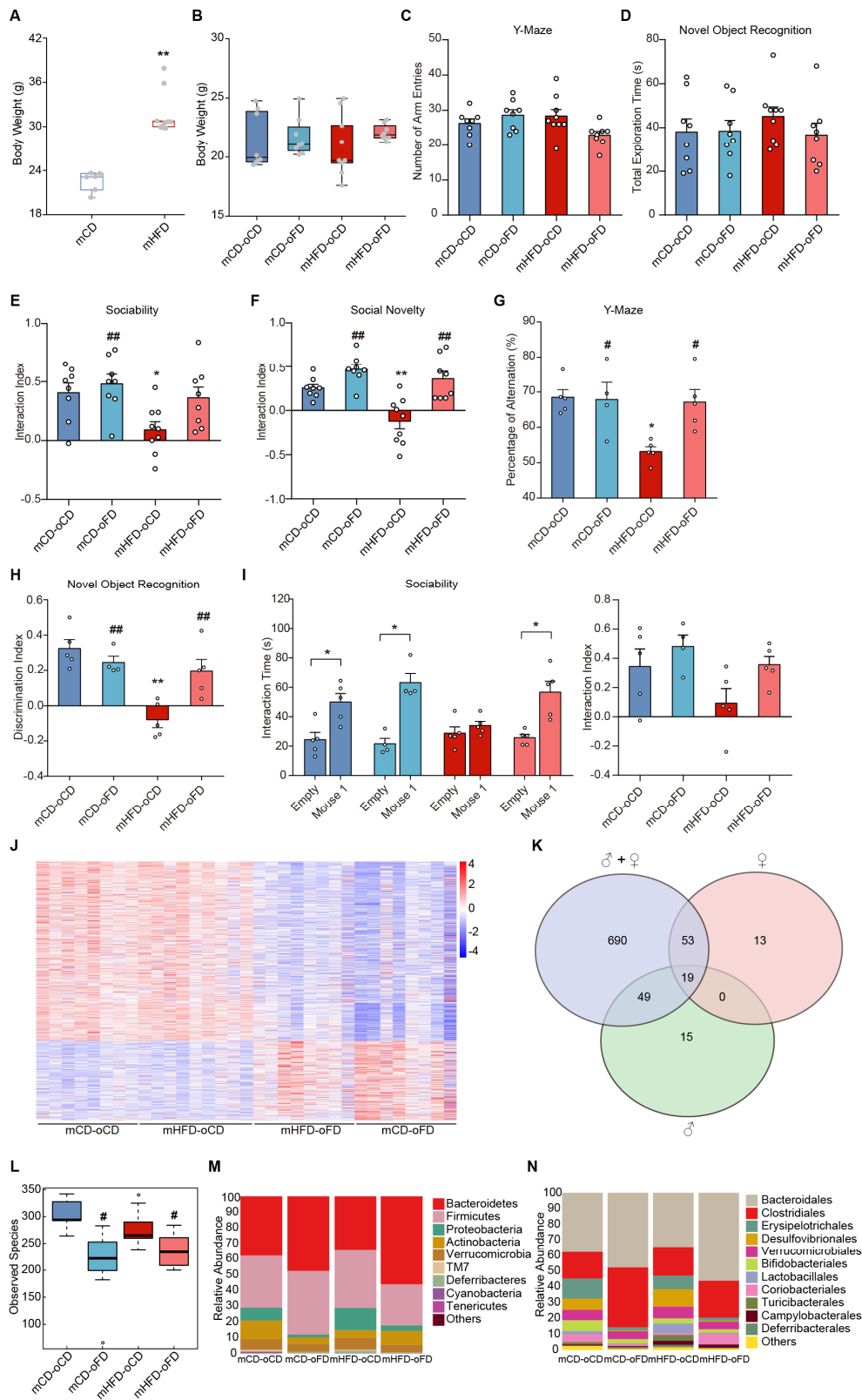


Figure S6 Offspring Dietary Fiber Intake Restored Maternal Obesity-induced Gene Changes in the Hippocampus and Microbiota Depletion, Related to Figures 4 and 5

(A) Body weight of dams after 12 weeks on a high-fat diet.

(B) Offspring weight at 8 weeks.

(C) The total number of arm entries of offspring after dietary fiber administration in the Y-maze test.

(D) Total exploration time of offspring after direct dietary fiber administration in the novel object recognition test.

(E-F) The index of sociability (E) and social novelty preference (F) in the three-chamber test.

(G-I) When all offspring within the same litter were considered as $n=1$, behavioral phenotypes in offspring after direct dietary fiber administration, including (G) Y-maze, (H) the novel object recognition test, and (I) sociability.

(J) Heatmap of the differentially expressed genes (DEGs) of the hippocampus using Ballgown software (FDR- $p < 0.05$).

(K) Overlap of the DEGs between sex combinations.

(L) α -Diversity in offspring, as measured by observed operational taxonomic units (OTUs). Differences between the treatment groups were tested using the Wilcoxon rank-sum test.

(M-N) The relative abundance of bacteria (M) at the phylum level and (N) at the order level in offspring.

Data shown in (A-B, and L) are presented as the median \pm interquartile range. Data shown in (C-I) are presented as the mean \pm SEM. (B-F and J-N) mCD-oCD n=8 mice, 5 litters; mCD-oFD n=8 mice, 4 litters; mHFD-oCD n=9 mice, 5 litters; mHFD-oFD n=8 mice, 5 litters. The gut microbiome of mHFD-oCD and mCD-oCD group in Figures 2, 5, S4, and S6 are from same mouse fecal samples. Statistical analyses were performed by using two-tailed Student's t-tests (for A) or by using a one-way ANOVA with Tukey's multiple comparison test (for B-I). For B-I, * p <0.05, ** p <0.01, compared with the mCD-oCD group, # p <0.05, ## p <0.01 versus the mHFD-oCD group.

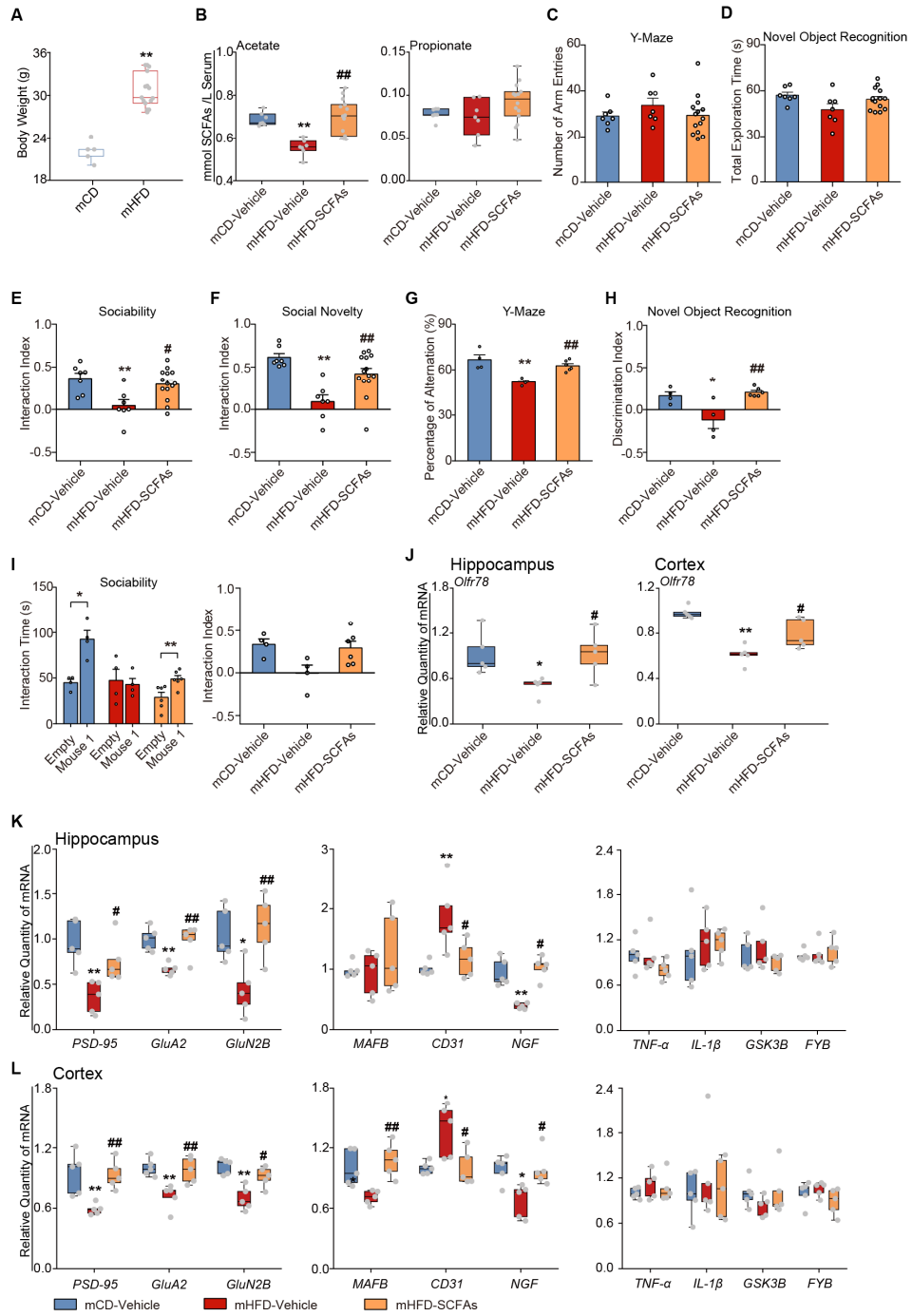


Figure S7 SCFAs Supplementation Restored Maternal Obesity-induced Cognitive Behavioral Deficits in Offspring, Related to Figure 6

(A) Body weight of dams.

(B) The concentrations of acetate (left) and propionate (right), in the offspring serum after treatment with a mixture of acetate and propionate.

(C) The total number of arm entries of offspring in the Y-maze test.

(D) Total exploration time of offspring in the novel object recognition test.

(E-F) The index of sociability (E) and social novelty preference (F) in the three-chamber test.

(G-I) When all offspring within the same litter were considered as $n=1$, behavioral phenotypes in offspring, including (G) Y-maze, (H) the novel object recognition test, and (I) sociability.

(J) The mRNA expressions of *Olf78* in the hippocampus (left) and prefrontal cortex (right).

(K) The mRNA expressions of levels of synapse-, microglia maturation-, and microglia function- related genes in the hippocampus.

(L) The mRNA expressions of levels of synapse-, microglia maturation-, and microglia function- related genes in the prefrontal cortex.

Data shown in (A-B) and (J-L) are presented as the median \pm interquartile range.

Data shown in (C-I) are presented as the mean \pm SEM. (B-F) mCD-Vehicle $n=7$ mice, 4 litters; mHFD-Vehicle $n=7$ mice, 4 litters; mHFD-SCFAs $n=14$ mice, 6 litters. (J-L) $n=5$ mice/group, 5 litters/group. Statistical analyses were performed

by using two-tailed Student's t-tests (for A) or by using a one-way ANOVA with Tukey's multiple comparison test (for B-L). For B-L, * $p < 0.05$, ** $p < 0.01$, compared with the mCD-Vehicle group, # $p < 0.05$, ## $p < 0.01$ versus the mHFD-Vehicle group.

SUPPLEMENTAL TABLE

Table S3. List of Primers, Related to KEY RESOURCES TABLE

Primers	Source	Identifier
The universal bacteria-Seq 8F: AGAGTTTGATCCTGGCTCAG	(Xiao et al., 2017)	N/A
The universal bacteria-Seq 338R: CTGCTGCCTCCCGTAGGAGT	(Xiao et al., 2017)	N/A
Bacterial hypervariable V3–V4 region of 16S rRNA-Seq 341_F: 5'-ACTCCTACGGGAGGCAGCAG-3'	European Nucleotide Archive, accession Number PRJEB31652	N/A
Bacterial hypervariable V3–V4 region of 16S rRNA-Seq 806_R: 5'-GGACTACHVGGGTWTCTAAT-3'	European Nucleotide Archive, accession Number PRJEB31652	N/A
<i>FXR1</i> -Seq (forward) 5'-GAGAGACTCGACATCAGCGA-3'	(Guo et al., 2015)	N/A
<i>FXR1</i> -Seq (reverse) 5'-AGTGTCTGCAGTCTGATCGG-3'	(Guo et al., 2015)	N/A
<i>GluA2</i> -Seq (forward) 5'-AAAGAATACCCTGGAGCACAC-3'	(Cook et al., 2014)	N/A
<i>GluA2</i> -Seq (reverse) 5'-CCAAACAATCTCCTGCATTTCC-3'	(Cook et al., 2014)	N/A
<i>PSD-95</i> -Seq (forward) 5'-TCTGTGCGAGAGGTAGCAGA-3'	(Martin et al., 2017)	N/A
<i>PSD-95</i> -Seq (reverse) 5'-AAGCACTCCGTGAACTCCTG-3'	(Martin et al., 2017)	N/A
<i>BDNF</i> -Seq (forward) 5'-CTGGATGAGGACCAGAAG-3'	(Sunkaria et al., 2017)	N/A
<i>BDNF</i> -Seq (reverse) 5'-CCTCCAGCAGAAAGAGTAG-3'	(Sunkaria et al., 2017)	N/A
<i>MAFB</i> -Seq (forward) 5'-GACAGGCTTTGCGTCCTAAG-3'	(Raverdeau et al., 2012)	N/A
<i>MAFB</i> -Seq (reverse) 5'-CGTTAGTTGCCAATGTGTGG-3'	(Raverdeau et al., 2012)	N/A
<i>CD31</i> -Seq (forward) 5'-ACTTCTGAACTCCAACAGCGA-3'	(Shimizu et al., 2017)	N/A
<i>CD31</i> -Seq (reverse) 5'-CCATGTTCTGGGGGTCTTTAT-3'	(Shimizu et al., 2017)	N/A
<i>CSF1R</i> -Seq (forward) 5'-GTCCACGGCTCATGCTGAT-3'	(Walter and Crews, 2017)	N/A
<i>CSF1R</i> -Seq (reverse) 5'-GTGAGTACAGGCTCCCAAGAG-3'	(Walter and Crews, 2017)	N/A

<i>F4/80</i> -Seq (forward) 5'-CGCTGCTGGTTGAATACAGAGA-3'	(Davies et al., 2008)	N/A
<i>F4/80</i> -Seq (reverse) 5'CGGTTGAGCAGACAGTGAATGA-3'	(Davies et al., 2008)	N/A
<i>CX3CL1</i> -Seq (forward) 5'-CAACTCCGAGGCACAGGAT-3'	(Walter and Crews, 2017)	N/A
<i>CX3CL1</i> -Seq (reverse) 5'-CCAAACGGTGGTGGAGATGT-3'	(Walter and Crews, 2017)	N/A
<i>CX3CR1</i> -Seq (forward) 5'-TCTTCACGTTCCGGTCTGGTG-3'	(Walter and Crews, 2017)	N/A
<i>CX3CR1</i> -Seq (reverse) 5'-TGCACTGTCCGGTTGTTTCAT-3'	(Walter and Crews, 2017)	N/A
<i>NGF</i> -Seq (forward) 5'-CGACTCCAAACACTGGAACTCA-3'	(Liu et al., 2017)	N/A
<i>NGF</i> -Seq (reverse) 5'-GCCTGCTTCTCATCTGTTGTCA-3'	(Liu et al., 2017)	N/A
<i>DAP12</i> -Seq (forward) 5'-CTGGTGCCTTCTGTTCCCTTC-3'	(Kaifu et al., 2003)	N/A
<i>DAP12</i> -Seq (reverse) 5'-CCTCTGTGTGTTGAGGTCAC-3'	(Kaifu et al., 2003)	N/A
<i>FXR2</i> -Seq (forward) 5'-TCAAGACCCCAGAGACGAAA-3'	(Guo et al., 2015)	N/A
<i>FXR2</i> -Seq (reverse) 5'-CTGAGGGTTTCGTGCGTTC-3'	(Guo et al., 2015)	N/A
<i>TDP2</i> -Seq (forward) 5'-CCCATACTGTGCCTACCTAAAGA-3'	This paper	N/A
<i>TDP2</i> -Seq (reverse) 5'-ACTCACATTTACGCATAGCAGG-3'	This paper	N/A
<i>GluN2B</i> -Seq (forward) 5'-AAGCCTGGCATGGTCTTCTC-3'	(Kratsman et al., 2016)	N/A
<i>GluN2B</i> -Seq (reverse) 5'-AGGTTGGCCATGTTTTTGGC-3'	(Kratsman et al., 2016)	N/A
<i>TNF-α</i> -Seq (forward) 5'-CTCATGCACCACCATCAAGG-3'	(Zhang et al., 2020)	N/A
<i>TNF-α</i> -Seq (reverse) 5'-ACCTGACCACTCTCCCTTTG-3'	(Zhang et al., 2020)	N/A
<i>IL-1β</i> -Seq (forward) 5'-TGACGGACCCCAAAGATGA-3'	(Wang et al., 2019)	N/A
<i>IL-1β</i> -Seq (reverse) 5'-TCTCCACAGCCACAATGAGT-3'	(Wang et al., 2019)	N/A
<i>GSK3B</i> -Seq (forward) 5'-ACAACAGTGGTGGCAACTCC-3'	(Rydbirk et al., 2016)	N/A
<i>GSK3B</i> -Seq (reverse) 5'-TTCTTGATGGCGACCAGTTCT-3'	(Rydbirk et al., 2016)	N/A

<i>FYB</i> -Seq (forward) 5'-AAGTTGCAGGACAAAGCTCGCCT-3'	(Adachi et al., 2018)	N/A
<i>FYB</i> -Seq (reverse) 5'-TCCTCGTAGGTAGGTTTCGCTGCC-3'	(Adachi et al., 2018)	N/A
<i>Olf78</i> -Seq (forward) 5'- ACTGCGTCACGCTGCTGTCC-3'	(Pluznick et al., 2013)	N/A
<i>Olf78</i> -Seq (reverse) 5'- ATGTAGGACAAGGGTGATAGGA-3'	(Pluznick et al., 2013)	N/A
<i>GAPDH</i> -Seq (forward) 5'-TGGAGAAACCTGCCAAGTATGA-3'	(Liu et al., 2017)	N/A
<i>GAPDH</i> -Seq (reverse) 5'-TGGAAGAATGGGAGTTGCTGT-3'	(Liu et al., 2017)	N/A